Guest Editor: Albert Viggiano

MEASUREMENTS OF VOLATILE ORGANIC COMPOUNDS IN THE EARTH'S ATMOSPHERE USING PROTON-TRANSFER-REACTION MASS SPECTROMETRY

Joost de Gouw[1,2]* and Carsten Warneke[1,2]

[1]*Chemical Sciences Division, Earth System Research Laboratory, National Oceanic and Atmospheric Administration, Boulder, Colorado 80305*

[2]*Cooperative Institute for Research in Environmental Sciences, University of Colorado, Boulder, Colorado 80309*

Received 28 February 2006; received (revised) 29 May 2006; accepted 30 May 2006

Published online 7 December 2006 in Wiley InterScience (www.interscience.wiley.com) DOI 10.1002/mas.20119

Proton-transfer-reaction mass spectrometry (PTR-MS) allows real-time measurements of volatile organic compounds (VOCs) in air with a high sensitivity and a fast time response. The use of PTR-MS in atmospheric research has expanded rapidly in recent years, and much has been learned about the instrument response and specificity of the technique in the analysis of air from different regions of the atmosphere. This paper aims to review the progress that has been made. The theory of operation is described and allows the response of the instrument to be described for different operating conditions. More accurate determinations of the instrument response involve calibrations using standard mixtures, and some results are shown. Much has been learned about the specificity of PTR-MS from inter-comparison studies as well the coupling of PTR-MS with a gas chromatographic interface. The literature on this issue is reviewed and summarized for many VOCs of atmospheric interest. Some highlights of airborne measurements by PTR-MS are presented, including the results obtained in fresh and aged forest-fire and urban plumes. Finally, the recent work that is focused on improving the technique is discussed. © 2006 Wiley Periodicals, Inc., Mass Spec Rev 26:223–257, 2007

Keywords: *proton-transfer-reaction mass spectrometry; atmospheric measurements; volatile organic compounds*

I. INTRODUCTION

Volatile organic compounds (VOCs) in the Earth's atmosphere are emitted from a wide variety of natural and man-made sources (Brasseur, Orlando, & Tyndall, 1999; Hewitt, 1999). Globally, the largest sources are tropical and extra-tropical forests, which emit large quantities of VOCs such as isoprene, α- and β-pinene and methanol (Guenther et al., 1995, 2006). Biomass burning is a large source of VOCs worldwide (Crutzen & Andreae, 1990), and leads to emissions of numerous VOCs, including many oxygenated species (organic acids, carbonyls and multi-functional species), nitriles (HCN, CH_3CN), and aromatics (benzene, toluene) (Andreae & Merlet, 2001; Friedli et al., 2001). Biomass burning can occur either naturally, for example, in forest fires or it can be caused by human activities, for example the burning of forest to clear agricultural land or the burning of agricultural waste. The production, storage, and use of fossil fuels is a large anthropogenic source of VOCs such as alkanes, alkenes, and aromatics, and although it is a much smaller source on a global scale, these sources can easily dominate on regional scales. Finally, the production and use of solvents, paints, and many other (household) chemicals leads to the release of many different VOCs. The atmospheric emissions of these are poorly quantified, but small on the global scale.

In the atmosphere, VOCs are removed by photochemical and deposition processes on timescales varying from minutes to months (Atkinson & Arey, 2003). Photochemical reactions are dominated by those with the hydroxyl radical (OH) in the sunlit atmosphere, but also include photolysis, reactions with ozone and, during the night, with nitrate radicals (NO_3) (Warneke et al., 2004a). As a result of this photochemistry, oxygenated VOCs (OVOCs) are formed, which can undergo all of these same reactions (de Gouw et al., 2005; Lewis et al., 2005). The ultimate fate of VOCs include the continued oxidation to form carbon dioxide (CO_2), the uptake by atmospheric aerosol, and deposition at the Earth's surface either directly (dry deposition) or by uptake in rain droplets (wet deposition). The relative importance of these different loss mechanisms is poorly characterized at present. The atmospheric photo-oxidation of VOCs leads to two important byproducts in the lower atmosphere, ozone and organic aerosol, which have important consequences for air quality and climate. Both ozone and organic aerosol have direct health effects for humans, as they are harmful to our respiratory system. Ozone is a greenhouse gas, but also has an indirect effect on the Earth's climate: it is an important precursor of OH radicals, which limit the atmospheric lifetime of greenhouse gases such as methane. Organic aerosols are another important factor in the Earth's climate system, either directly through the scattering and absorption of sunlight, or indirectly by acting as condensation nuclei for cloud droplets (Novakov & Penner, 1993).

**Correspondence to:* Joost de Gouw, Chemical Sciences Division, Earth System Research Laboratory, National Oceanic and Atmospheric Administration, Boulder, CO 80305. E-mail: Joost.degouw@noaa.gov

Measurements of VOCs in the atmosphere have largely been done using gas chromatographic analyses of air samples that were either collected in canisters, on adsorbents or in cryostats. Such measurements are very sensitive and give a high degree of chemical detail: tens of VOCs with volume mixing ratios down to 0.1 pptv (parts-per-trillions by volume) can be determined from the samples. There are, however, several disadvantages to such methods. Using adsorbents and cryostats, a sampling time of several minutes is required to get enough sample material. As a consequence, in rapidly changing atmospheric conditions, GC measurements will not be able to follow those changes with a suitable response time. This may be the case close to emission sources or when sampling from a rapidly moving platform. This disadvantage can partially be overcome by using canister samples, which can be filled in several seconds. However, the acquisition and analysis of canister samples is time consuming and labor intensive, which still limits the amount of data that can be collected in any given period. In addition, not all VOCs are quantitatively retained in canisters. In summary, GC measurements provide highly detailed snapshots of the atmospheric VOC composition, but are generally too slow to follow rapid changes in air mass composition.

Proton-transfer-reaction mass spectrometry (PTR-MS) was developed by Professor Werner Lindinger and co-workers at the University of Innsbruck in Austria, and overcomes some of the disadvantages of GC methods at the cost of chemical detail (Lindinger, Hansel, & Jordan, 1998; Lindinger, Fall, & Karl, 2001). In PTR-MS, the air to be analyzed is continuously pumped through a drift tube reactor, and a fraction of the VOCs is ionized in proton-transfer reactions with hydronium ions (H_3O^+). The advantage of using proton transfer is that it is a soft ionization method, that is, it generally does not lead to fragmentation of the product ions, and the mass of the product ion equals the VOC mass plus one. At the end of the drift tube, the reagent and product ions are measured by a quadrupole mass spectrometer, and the product ion signal is proportional to the VOC mixing ratio. PTR-MS allows numerous VOCs of atmospheric interest to be monitored with a high sensitivity (10–100 pptv) and rapid response time (1–10 sec). In addition, the technique does not require any sample treatment such as drying or pre-concentration, and is thus well suited for oxygenated VOCs, which cannot be quantified from canister samples. A major disadvantage is that PTR-MS only determines the mass of product ions, which is of course not a unique indicator of the VOC identity. It is clear that isomers cannot be distinguished, and the interpretation of mass spectra is further complicated by the formation of cluster ions and the fragmentation of product ions. A significant experimental effort has therefore been made to characterize the specificity of PTR-MS for different VOCs in the Earth's atmosphere (de Gouw et al., 2003b; Warneke et al., 2003). In summary, PTR-MS provides a fast-response measurement of several key atmospheric VOCs, and complements the highly sensitive and chemically detailed snapshots obtained by GC techniques.

Proton-transfer-reaction mass spectrometry has been used since 1998 for field measurements of atmospheric VOCs from a wide variety of aircraft, ship- and ground-based platforms. Over the course of these years, much has been learned about the performance, instrument response and specificity of the instrument for VOCs in various regions of the atmosphere. It is the purpose of this paper to review this work, and also to highlight some of the research applications that were made possible through the development of PTR-MS. Previous reviews of PTR-MS focused on the design of the instrument and on some early applications in atmospheric, food, and medical research (Lindinger, Hansel, & Jordan, 1998; Lindinger, Fall, & Karl, 2001; Hewitt, Hayward, & Tani, 2003). Here, we will discuss in Section II the PTR-MS instrument and review what has been learned about the instrument response, detection limits and response time for different VOCs. In Section III we will discuss the specificity of PTR-MS for different VOCs, which was studied by combining a PTR-MS with a GC interface, and by comparing PTR-MS with alternative methods. In Section IV we will discuss some highlights of airborne research on atmospheric VOCs where the response time of PTR-MS is essential to get good data coverage. Finally, in Section V we will summarize some of the ongoing research to improve PTR-MS instruments. Not included in this review is a discussion of the so-called selected-ion flow tube mass spectrometry (SIFT-MS) technique (Smith & Spanel, 2005), which is similar to PTR-MS. In SIFT-MS, H_3O^+, NO^+, or O_2^+ ions from an ion source are mass-selected, injected into a flow tube reactor, and used to ionize VOCs. The use of ions other than H_3O^+ can be useful in the identification of VOCs. On the other hand, the reagent ion count rates and therefore the sensitivity are much lower than in PTR-MS. As a result, applications of SIFT-MS to atmospheric measurements have been very limited.

II. PROTON-TRANSFER-REACTION MASS SPECTROMETRY

A. Instrumental Set-Up

1. PTR-MS

Lindinger et al. discussed the design of the PTR-MS instrument in detail (Lindinger, Hansel, & Jordan, 1998; Lindinger, Fall, & Karl, 2001), and a shorter description is given here. Figure 1 gives a schematic drawing of the PTR-MS instrument in our laboratory, which was the first instrument built by Ionicon. The set-up consists of (1) a discharge ion source to produce the H_3O^+ ions, (2) a drift-tube reactor, in which the proton-transfer reactions between H_3O^+ and VOCs take place, and (3) a quadrupole mass spectrometer for the detection of reagent and product ions. Brief descriptions of all these elements follow below.

The ion source consists of a hollow cathode discharge in water vapor and provides an intense source of H_3O^+ ions. A constant flow of water vapor (0–20 STP cm^3/min) is supplied preferably using a low-Δp flow controller, which controls the flow coming from the headspace of a liquid water reservoir. In the small intermediate chamber, ions from the hollow-cathode are further converted into H_3O^+ ions while being transported towards the drift tube. By varying the voltages of the two elements that make up this chamber (V_4 and V_5; see Fig. 1), the H_3O^+ signal can be increased at the cost of producing a higher fraction of O_2^+ and NO^+ impurity ions. The latter are formed from air back streaming from the drift tube into the ion source, and are

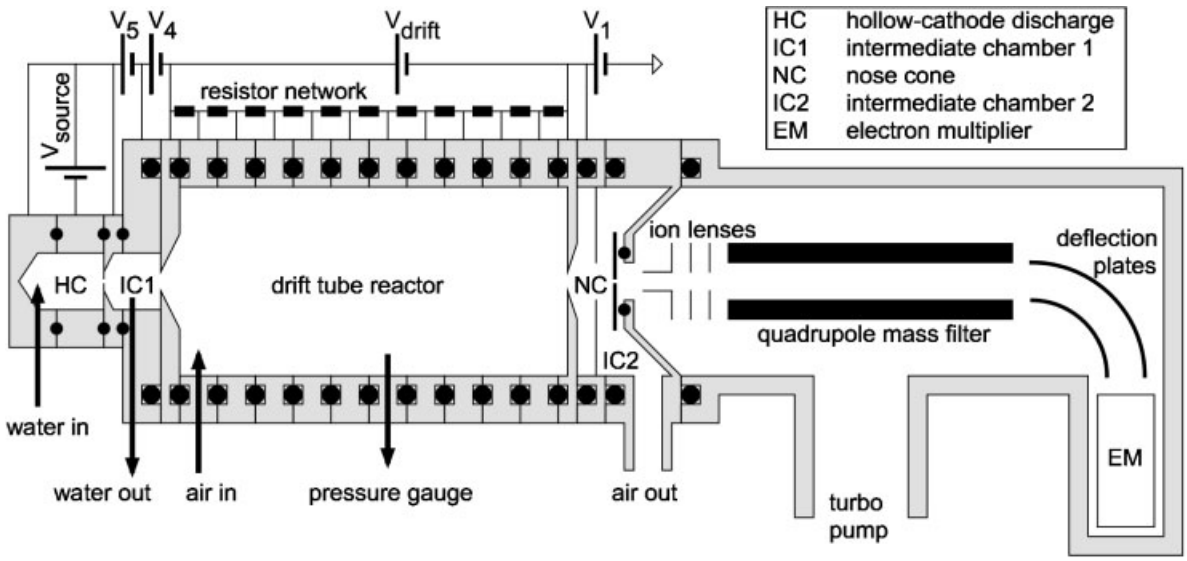

FIGURE 1. Schematic drawing of the PTR-MS instrument.

unwanted as they undergo charge-transfer reactions with most VOCs, which is a much harder ionization method for many VOCs including species such as alkanes that do not react with H_3O^+ (Arnold, Viggiano, & Morris, 1998).

The performance of the source is illustrated by Figure 2, which shows the dependence of the H_3O^+, O_2^+, and NO^+ signals on the voltages V_4 and V_5 (see Fig. 1). All ion signals increase with increasing V_4 and V_5. Increasing V_4 leads to a relative increase in the production of O_2^+ (from $<1\%$ at $V_4 = 80$ V to $>10\%$ at $V_4 = 170$ V; see Fig. 2A) and should be limited in practice. Increasing V_5, on the other hand, does not lead to a relative increase of O_2^+ (Fig. 2B). It should be noted that the results in Figure 2 depend on operating conditions such as the water vapor flow, the humidity of the sample air, the cleanliness of the source electrodes, etc., and probably differ quantitatively from instrument to instrument. The qualitative behavior, however, remains approximately the same.

The drift tube consists of a number of stainless steel rings that are separated by Teflon rings, which seal the vacuum and isolate the drift rings electrically. The drift rings are connected to a resistor network, which divides the overall drift voltage (V_{drift}; see Fig. 1) into a homogeneously increasing voltage and establishes a homogeneous electric field inside the reactor. Increasing the ion kinetic energy using the drift field limits the degree of cluster-ion formation and simplifies the interpretation of the mass spectra. As an added advantage, the electric field is also mostly responsible for the transport of ions over the length of the drift tube, as opposed to a flow tube in which the ions are transported by a fast flow of gas. The use of a drift tube thus eliminates the need for a large pump, which allows for a compact instrument design.

The drift tube is separated from the second intermediate chamber by a small orifice, and most of the air is pumped away by a turbo pump. A fraction of the ions is extracted through the nose cone into the quadrupole mass spectrometer, which consists of a commercial Pfeiffer Vacuum QMA 400 mass filter and an electron multiplier for ion pulse counting. In most experiments,

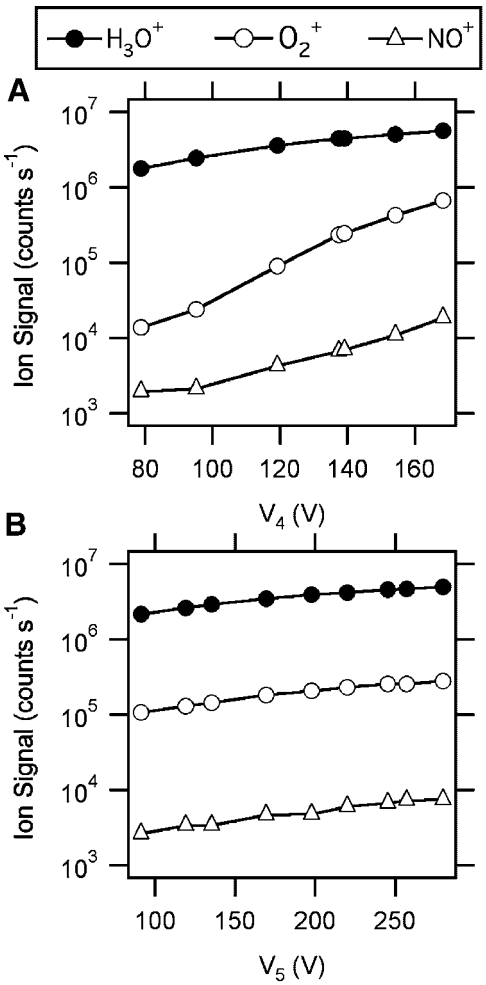

FIGURE 2. Dependence of the primary ion signals on the voltages V_4 and V_5 in the ion source. The measurements were done with a water vapor flow of 6.6 STP cm^3/min and with dry, clean air sampled into the drift tube.

the mass spectrometer is run in selected-ion mode, in which the mass filter steps between certain ions of interest rather than scans over a range of masses.

Ionicon has built different versions of PTR-MS instruments with relatively minor but nonetheless important differences from the instrument described above. In an attempt to improve the response time of the instrument, the diameter and volume of the drift tube were reduced to decrease the residence time of air. Another important modification involved the addition of a second intermediate vacuum chamber in between the drift tube and the quadrupole MS, which is pumped by a third turbo pump. As a result, the sampling orifice in front of the quadrupole could be enlarged and higher ion detection efficiencies were obtained. Finally, Ionicon has designed a compact version of the PTR-MS based on the Prisma mass spectrometer from Pfeiffer Vacuum. As opposed to the PTR-MS instrument described above, the Prisma uses ion current detection rather than pulse counting, which results in poorer detection limits. The applicability for atmospheric measurements is probably limited.

2. Gas Inlet System

The purpose of the gas inlet system is to supply the drift tube with a constant flow of air at a constant pressure, regardless of the ambient atmospheric pressure. The latter is especially important in aircraft measurements, where the ambient pressure depends on the flight altitude. The second design consideration is to minimize wall losses of VOCs, which is achieved by exposing the sample air only to perfluoro alkoxy (PFA), PTFE Teflon and/or silco-steel.

A schematic diagram of the inlet system used in our laboratory is shown in Figure 3. A diaphragm pump pulls air into the inlet, and a pressure controller controls the inlet flow between 20 and 500 STP cm^3/min, such that the pressure upstream from the pressure controller is kept constant (100–200 mbar). A Teflon needle valve, mounted upstream of the pressure controller, introduces a flow restriction to the inlet and thus limits the flow that is needed to drop the pressure to the required value. From the pressure controller a narrow-bore Teflon tube leads to the drift tube, and this flow restriction limits the flow and drops the pressure further down to the drift tube pressure of 2.0–2.4 mbar. Instead of the narrow-bore tube a critical orifice can also be used.

The inlet flow can be diverted through a catalytic converter to determine the background signals in the system. The catalytic converter consists of Platinum wool (Shimadzu, high sensitivity catalyst for TOC analyzer) heated to 350°C and efficiently removes VOCs from the inlet flow, but does not change the humidity, as a charcoal filter or adding zero air would. This is important because some of the background signals depend on the ambient humidity. Examples are presented in Figure 4, which shows the background mixing ratios of four VOCs measured during a research flight, as a function of the measured ratio between $H_3O^+(H_2O)$ and H_3O^+ ions. The latter can be used as a proxy for the ambient humidity, as will be seen below. For some VOCs the background does not depend strongly on the humidity, such as for acetonitrile (Fig. 4B). For many species, such as toluene (Fig. 4D), the background increases with humidity: humid air seems to ''flush'' more impurities from the walls of the inlet system than dry air. Finally, for methanol and methyl ethyl ketone (MEK), the backgrounds depend strongly on the humidity because it influences the ion chemistry in the drift tube. In the case of methanol, an important contribution to the background is from $^{16}O^{17}O^+$ ions, which decrease with increasing humidity (Fig. 4A): O_2^+ reacts with H_2O albeit slowly in a multi-step reaction (Good, Durden, & Kebarle, 1970). In the case of MEK, most of the background consists of $H_3O^+(H_2O)_3$ cluster ions, which increase with increasing humidity (Fig. 4C). During an ambient air measurement, regular background measurements are made, which are subtracted from the signal without catalyst to get ambient VOC concentrations. This is of particular importance for aircraft measurements, during which the humidity can change rapidly as a function of flight altitude. In addition, the operation

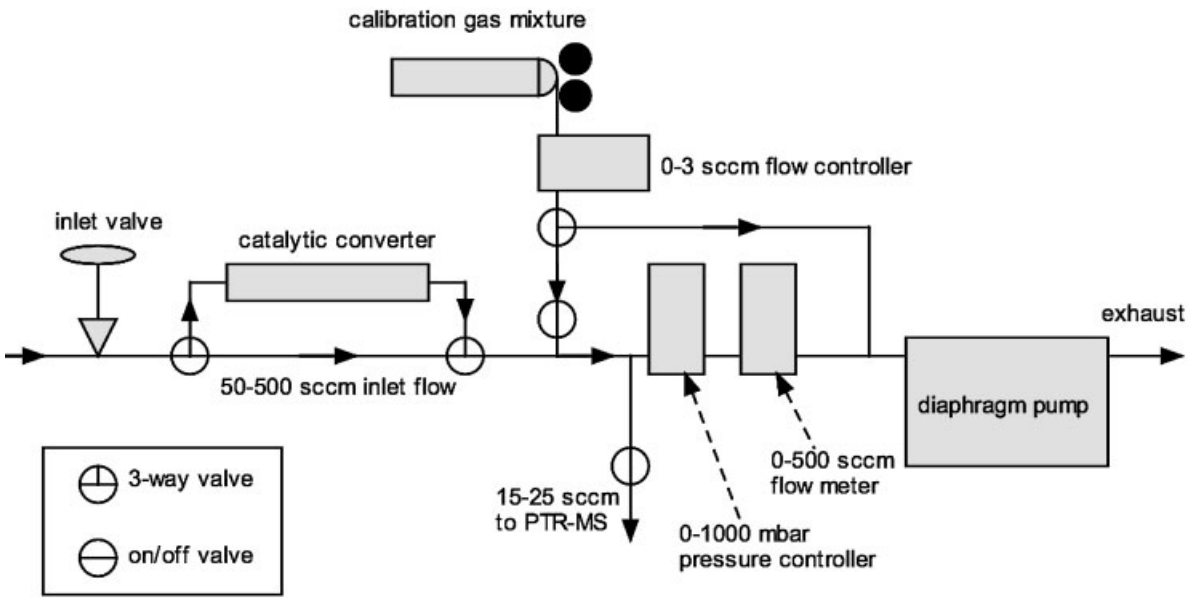

FIGURE 3. Schematic drawing of the gas inlet system.

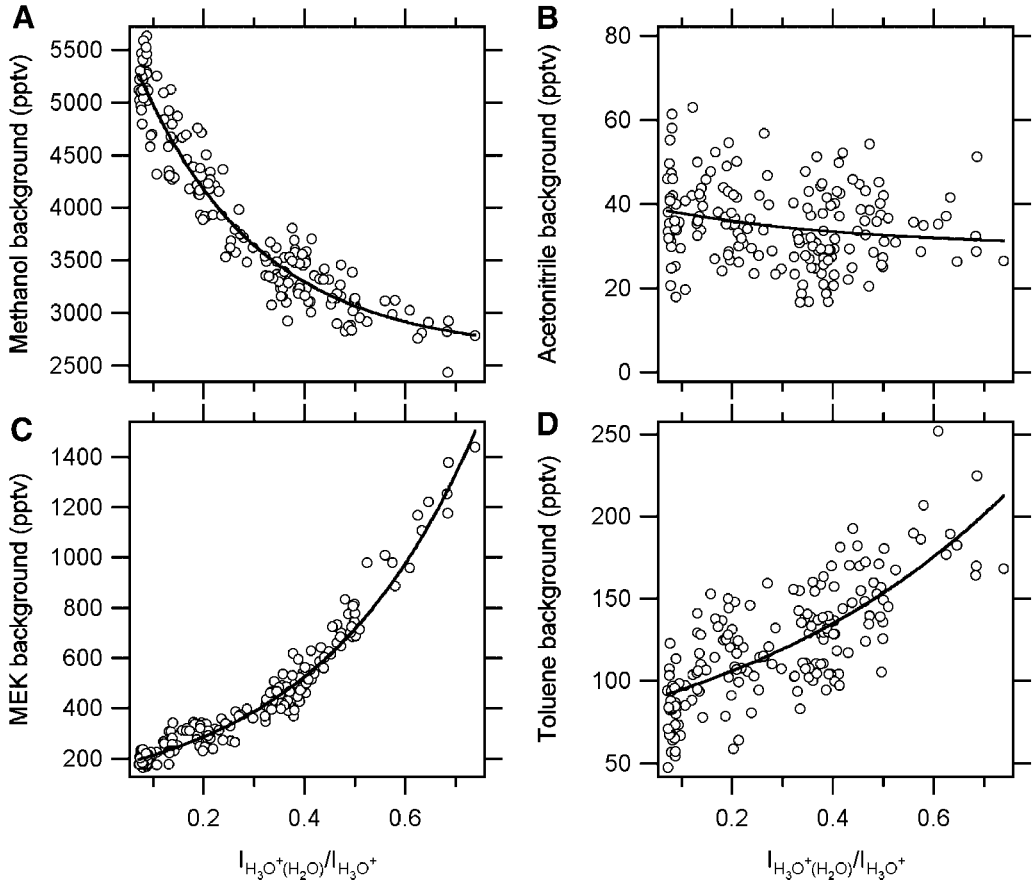

FIGURE 4. Dependence of the instrument backgrounds for (**A**) methanol, (**B**) acetonitrile, (**C**) MEK, and (**D**) toluene on the measured ratio between $H_3O^+(H_2O)$ and H_3O^+ ions, which is a proxy for the ambient humidity.

of PTR-MS systems onboard aircraft often involves starting up the instrument only shortly before a flight. As a result, the system backgrounds are not as low as they can be after several days of continuous operation, and background levels can decrease during a flight.

A calibration gas mixture can be added to the inlet for calibration purposes (Fig. 3). The calibration gas flow is regulated by a flow controller (0–3 STP cm^3/min), and the flow is either added to the inlet or directed into an exhaust pump. The flow of calibration gas can thus be kept constant, which gives the most accurate results: it allows the pressure reducer and flow controller to equilibrate with the calibration gas composition even when no calibrations are made. This is important as it can take up to several days for some species, for example methanol, to yield stable calibration measurements with this set-up (de Gouw et al., 2003a).

B. Ion Chemistry in the Drift Tube

1. Proton-Transfer Reactions

In PTR-MS, proton-transfer reactions with H_3O^+ ions are used to ionize trace gases *R* in air

$$H_3O^+ + R \rightarrow RH^+ + H_2O \qquad (2.1)$$

These reactions are exothermic if the proton affinity (PA) of *R* is higher than the PA of water (166.5 kcal/mol), in which case the reaction proceeds at a rate close to the collision rate of a few times 10^{-9} cm^3/molecule/sec. A relatively recent compilation of proton affinities was given by Hunter and Lias (1998). Atmospheric trace gases that react with H_3O^+ include unsaturated and aromatic hydrocarbons, and also most of the oxygenated VOCs (aldehydes, ketones, alcohols, acids, etc.). Numerous studies (Barker & Ridge, 1976; Chesnavich, Su, & Bowers, 1980; Su & Chesnavich, 1982) have shown how the collision rate coefficient for reaction (2.1) can be calculated from the polarizability and permanent dipole moment of the molecule *R* (Lide, 2005).

Due to the advent of PTR-MS and the related SIFT-MS technique, there has been a lot of recent work on the kinetics and products of reaction (2.1). For example, Smith and co-workers studied proton-transfer between H_3O^+ and aldehydes and ketones (Spanel, Ji, & Smith, 1997; Spanel, Van Doren, & Smith, 2002), alcohols (Spanel & Smith, 1997), acids (Spanel & Smith, 1998b), aromatics (Spanel & Smith, 1998a), alkenes (Diskin et al., 2002), monoterpenes (Wang, Spanel, & Smith, 2003), peroxyacetic acid (Spanel et al., 2003), and hydrogen cyanide (Spanel, Wang, & Smith, 2004). Viggiano and co-workers studied proton-transfer between H_3O^+ (and $H_3O^+(H_2O)$ ions) with alkanes (Arnold, Viggiano, & Morris, 1998),

formaldehyde and acetaldehyde (Midey, Arnold, & Viggiano, 2000) and alkyl benzenes (Midey et al., 2002). A thorough review of this work is beyond the scope of this paper. A recent compilation of rate coefficients for reaction (2.1) was included in a report from the Jet Propulsion Laboratory (Anicich, 2003). Finally, Zhao and Zhang published proton-transfer rate coefficients for a range of VOCs that were calculated using quantum chemical methods (Zhao & Zhang, 2004).

For VOCs that have a PA only slightly higher than that of water, the exothermicity of reaction (2.1) is small and the rate coefficient of the reverse reaction

$$RH^+ + H_2O \rightarrow H_3O^+ + R \qquad (2.2)$$

is non-negligible. This is the case, for example, for formaldehyde. The rate coefficient for the reverse reaction is several orders of magnitude lower than that of the forward reaction, but since the concentration of H_2O in the drift tube is much higher than the concentration of *R*, the overall rate of the forward and backward reactions can be comparable. As a result, the proton-transfer between H_3O^+ and VOCs such as formaldehyde is less efficient, and moreover, the overall rate depends on the humidity of the sampled air. The kinetics of the forward and backward reaction for formaldehyde have been measured in a selected-ion flow drift tube experiment (Hansel et al., 1997), but no experimental studies on the humidity dependence of the formaldehyde detection by PTR-MS have been published.

The RH^+ ions produced from reaction (2.1) can undergo fragmentation, and some examples will be shown in the next section for alkyl benzenes and monoterpenes. The fragmentation of several monoterpenes was investigated as a function of the humidity of the sampled air and the operating conditions of the drift tube (Tani et al., 2004). Apart from this study, very little systematic research into product ion fragmentation has been reported, but would be very useful in the interpretation of PTR-MS data.

2. Cluster Ion Formation and Chemistry

In addition to reaction (2.1), the H_3O^+ and RH^+ ions can cluster with water molecules in the sampled air (Lau, Ikuta, & Kebarle, 1982):

$$H_3O^+ + n\,H_2O \leftrightarrow H_3O^+(H_2O)_n \qquad (2.3)$$

$$RH^+ + n\,H_2O \leftrightarrow RH^+(H_2O)_n \qquad (2.4)$$

These cluster ions are a problem because their presence complicates the interpretation of the mass spectra. In PTR-MS, cluster ion formation is effectively reduced by enhancing the kinetic energy of the reagent ions. This is accomplished with an electric field over the length of the drift tube. However, depending on the electric field and pressure in the drift tube, $H_3O^+(H_2O)$ cluster ions can still be present in the drift tube and react by (Midey, Arnold, & Viggiano, 2000; Midey et al., 2002)

$$H_3O^+(H_2O) + R \rightarrow RH^+ + 2H_2O \qquad (2.5)$$

This reaction probably occurs either directly, by proton-transfer, or indirectly by ligand exchange and rearrangement of the product ions. For most VOCs, reaction (2.5) is approximately as efficient as reaction (2.1). The exceptions include (i) species with a low PA, since the PA of $(H_2O)_2$ clusters is higher than that of H_2O, and (ii) species with a low polarity. In cases where the concentrations of $H_3O^+(H_2O)$ and H_3O^+ ions in the drift tube are of the same order of magnitude, the sensitivity of PTR-MS is determined by reactions (2.1) and (2.5). For compounds like benzene and toluene that do not react with $H_3O^+(H_2O)$ the sensitivity will only be determined by reaction (2.1) (Warneke et al., 2001b). For these compounds, the concentrations of $H_3O^+(H_2O)$ and H_3O^+ ions and therefore the sensitivity depend on the humidity of the sampled air. We will show further below how the RH^+ ion signals can be normalized to the signals of $H_3O^+(H_2O)$ and H_3O^+ ions, such that humidity effects are taken into account.

The $RH^+(H_2O)$ ions produced in reaction (2.4) can interfere with the detection of higher mass species, and examples will be shown for the detection of dimethyl sulfide (DMS). The $H_3O^+(H_2O)$ ion bond energy is relatively high, and therefore the ratio between $RH^+(H_2O)$ and RH^+ ions is typically lower than between $H_3O^+(H_2O)$ and H_3O^+ ions. Few systematic studies of $RH^+(H_2O)$ cluster ion formation have been reported, but would be very useful in the interpretation of PTR-MS data.

To limit the degree of cluster ion formation, an electric field is applied over the length of the drift tube. As a result, the ions move with an average drift velocity v_d

$$v_d = \mu \times E \qquad (2.6)$$

where μ is the ion mobility and E the electric field. The ion mobility has been measured for numerous ions in different gases, including for H_3O^+ ions in nitrogen (Dotan et al., 1976; Viehland & Mason, 1995). Generally, the reduced mobility μ_0 is reported

$$\mu_0 = \frac{p}{p_0} \times \frac{T_0}{T} \times \mu = \frac{N}{N_0} \times \mu \qquad (2.7)$$

In this equation, p is the pressure, T the temperature, and N the number density of the gas in the drift tube. The parameter N_0 is the gas number density at standard pressure p_0 (1 atm) and temperature T_0 (273.15 K). The drift velocities of H_3O^+ and $H_3O^+(H_2O)$ ions in the PTR-MS have been measured (Warneke et al., 2001b). Even though the mobilities of H_3O^+ and $H_3O^+(H_2O)$ ions in N_2 are different (Dotan et al., 1976; Viehland & Mason, 1995), they were measured to be the same in the PTR-MS drift tube, and equal to the average of the mobilities of H_3O^+ and $H_3O^+(H_2O)$ ions, weighted by their relative abundance in the drift tube. This reflects the fact that reactions (2.3) are in equilibrium: each ion binds with and loses an H_2O ligand many times while traversing the length of the drift tube (Warneke et al., 2001b).

Substituting (Eq. 2.7) into (2.6) gives

$$v_d = \mu_0 N_0 \times (E/N) \qquad (2.8)$$

This equation shows that the drift velocity is a function of the parameter *E*/*N*, which is frequently used in ion mobility studies and is expressed in units of Townsend (1 Td = 10^{-17} V cm^2).

Using the drift velocity v_d, an effective ion temperature T_{eff} can be defined as (de Gouw et al., 2003b)

$$\frac{3}{2}k_B T_{eff} = \frac{1}{2}m_b v_d^2 + \frac{3}{2}k_B T \quad (2.9)$$

This equation is a modified version of the Wannier expression (Viggiano & Morris, 1996), in which m_b is the molecular mass of the "buffer" gas; in this case air. Using T_{eff}, the equilibrium constants for reactions (2.3) (Lau, Ikuta, & Kebarle, 1982) and the concentration of water vapor in the drift tube, the distribution of $H_3O^+(H_2O)_n$ cluster ions can be calculated (de Gouw et al., 2003b). The first term on the right-hand side of Equation (2.9) usually dominates and thus T_{eff} is typically much higher than T. This shows in combination with Equation (2.8) that the cluster ion distribution in the drift tube is largely determined by the parameter E/N.

The effects of the parameter E/N on the cluster ion distribution is demonstrated in Figure 5, which shows the signal and distribution of $H_3O^+(H_2O)_n$ ions in the drift tube as a function of the drift field and the parameter E/N. H_3O^+ ions dominate above a drift voltage of ~600 V, $H_3O^+(H_2O)$ ions dominate between ~350 and ~600 V, and $H_3O^+(H_2O)_2$ ions dominate below ~350 V. The total signal is constant to within a factor of 2 over the entire range. Also shown are the fractions calculated using: (i) the effective ion temperature T_{eff}, (ii) the equilibrium constants for reactions (2.3) (Lau, Ikuta, & Kebarle, 1982), and (iii) the concentration of water vapor in the drift tube. It is seen that the calculated distribution describes the dependence on E/N only semi-quantitatively. The reasons for the discrepancies have not been investigated in detail, but may include: (1) Equation (2.9) ignores the kinetic and internal energy of the neutrals at the temperature of the drift tube, (2) the assumption that the velocity distribution is Maxwellian may not be valid, (3) each ion has a different temperature according to Equation (2.9) because of their different mobilities, (4) the measured cluster ion distribution does not exactly reflect the actual ion distribution in the drift tube (Warneke et al., 2001b), and (5) the water vapor concentration inside the drift tube is not known exactly.

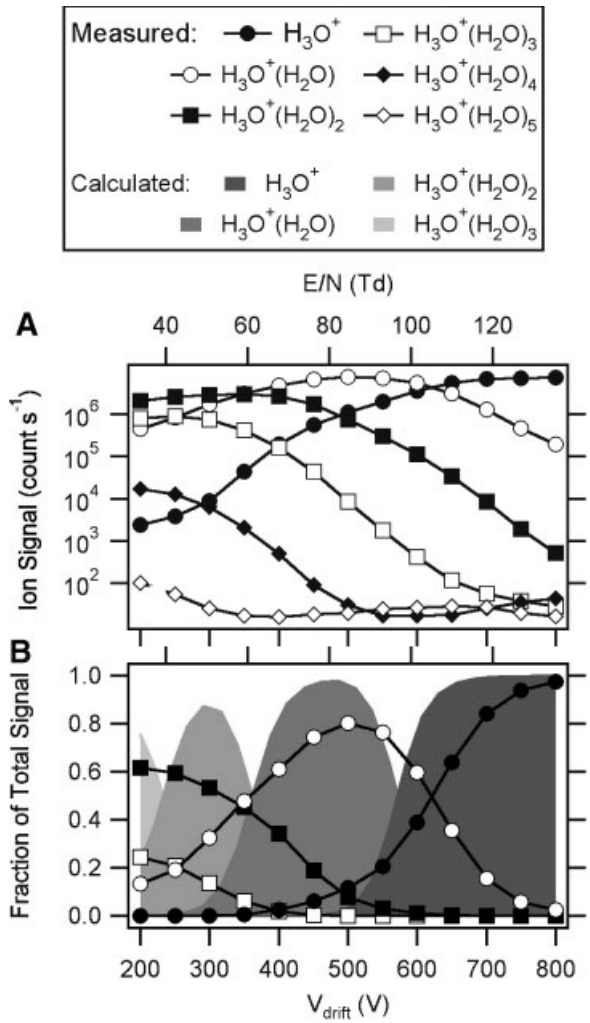

FIGURE 5. Signal and distribution of $H_3O^+(H_2O)_n$ ions in the drift tube as a function of the drift field (V_{drift}) on the bottom axis, and on the top axis the parameter E/N, calculated from V_{drift} and the pressure (2.4 mbar) and temperature (298 K) of the drift tube. **Panel A** shows the ion signals on a logarithmic scale; **panel B** shows the fraction of the signal compared with a model calculation.

C. Calibrations and Detection Limits

1. Calculation of Sensitivities

The concentration of H_3O^+ ions after traversing the drift tube with the reaction time Δt can be described as

$$[H_3O^+]_{\Delta t} = [H_3O^+]_0 \exp(-k[R]\Delta t) \quad (2.10)$$

In this equation, $[H_3O^+]_0$ is the concentration of reagent ions injected from the ion source, k is the rate coefficient for the proton-transfer reaction (2.1), and (R) is the concentration of trace gas R. It is assumed that the only loss of reagent ions occurs through reaction (2.1). In reality, the radial diffusion of ions and collisions with the wall of the drift tube leads to additional losses. It can be shown, however, that such losses are relatively small in the PTR-MS under the operating conditions that are normally used. Also, it is assumed in Equation (2.10) that there is only one trace gas R reacting with H_3O^+. If more trace gases are present, as in any air sample, the term $k[R]\Delta t$ in Equation (2.10) has to be replaced with $\Sigma\, k_i[R_i]\Delta t$, where the summation is made over all the different trace gases. The concentration of RH^+ ions produced from reaction (2.1) is given by

$$[RH^+] = [H_3O^+]_0\{1 - \exp(-k[R]\Delta t)\} \approx [H_3O^+]k[R]\Delta t \quad (2.11)$$

The approximation in Equation (2.11) is justified if $k[R]\Delta t$ is small, in other words if only a small fraction of H_3O^+ ions reacts in the drift tube. Equation (2.11) shows that under these conditions the density of RH^+ ions at the end of the drift tube is linear in the concentration of the trace gas R.

The reaction time Δt is determined by the ion drift velocity Equation (2.8)

$$\Delta t = \frac{L}{\mu_0 N_0} \times (E/N)^{-1} \tag{2.12}$$

where L is the length of the drift tube ($\sim$10 cm). Using Equations (2.11) and (2.12), the fraction of H_3O^+ ions that is converted into RH^+ ions can be expressed as

$$\frac{[RH^+]}{[H_3O^+]} = [R] \times \frac{kL}{\mu_0 N_0} \times (E/N)^{-1} \tag{2.13}$$

where $[R]$ is the concentration of trace gas R in the drift tube. A fraction of H_3O^+ and RH^+ ions is sampled into the quadrupole mass spectrometer and detected by the electron multiplier. The count rates observed, $I_{H_3O^+}$ for H_3O^+ and I_{RH^+} for RH^+ ions, are related to the quantity to be determined, the volume-mixing ratio VMR (=$[R]/N$), by

$$\begin{aligned} \frac{I_{RH^+}}{I_{H_3O^+}} &= \frac{[RH^+]}{[H_3O^+]} \times \frac{T_{RH^+}}{T_{H_3O^+}} \\ &= \text{VMR} \times \frac{kL}{\mu_0 N_0} \times \frac{N^2}{E} \times \frac{T_{RH^+}}{T_{H_3O^+}} \end{aligned} \tag{2.14}$$

In this equation the factors T_{RH^+} and $T_{H_3O^+}$ are the transmission efficiencies for RH^+ and H_3O^+ ions, respectively, and are determined by (i) the extraction efficiency of ions from the drift tube into the quadrupole, (ii) the transmission efficiency of the quadrupole mass spectrometer, and (iii) the detection efficiency of the electron multiplier for each mass. The largest mass-dependent differences are introduced by the quadrupole mass spectrometer. The ratio $T_{RH^+}/T_{H_3O^+}$ can be determined experimentally, for instance by adding a single compound R and by measuring the decrease in the H_3O^+ signal simultaneously with the increase in RH^+ signal (Ammann et al., 2004; Steinbacher et al., 2004). From Equation (2.14), we define the sensitivity as the signal of RH^+ ions obtained at a VMR of 1 ppbv (parts per billion by volume: 10^{-9}) and normalized to a H_3O^+ signal ($I_{H_3O^+}$) of 10^6 counts/sec

$$\text{Sensitivity} = 10^{-3} \times \frac{kL}{\mu_0 N_0} \times \frac{N^2}{E} \times \frac{T_{RH^+}}{T_{H_3O^+}} \tag{2.15}$$

The sensitivity is expressed in units of normalized counts/sec/ppbv (ncps/ppbv).

Transmission curves of the mass spectrometer in a PTR-MS show a lower transmission for H_3O^+ than for ions above 40 amu (Ammann et al., 2004; Steinbacher et al., 2004). Steinbacher et al. reported differences of up to 25% between the measured transmission curve and the curve recommended by Ionicon. When using the calculated sensitivity Equation (2.15), the accuracy is limited by the uncertainties in (i) the rate coefficient k, which can be up to 50%, and (ii) the ratio $T_{RH^+}/T_{H_3O^+}$, which can be 25%. A comparison between calculated and measured sensitivities indeed shows differences of up to a factor of 2 (Warneke et al., 2003). For atmospheric measurements a higher accuracy is generally required, and the accuracy can be improved by calibrating the instrument using standard mixtures of VOCs in air or nitrogen.

2. *Calibrations*

Figure 6 illustrates the effect of the humidity of the sampled air on the sensitivities as described earlier. The figure shows the ion signals observed for H_3O^+ (19 amu), $H_3O^+(H_2O)$ (37 amu), protonated acetone (59 amu) and protonated toluene (93 amu) as a function of the humidity of the sampled air. We estimated that $\sim$5% of the water flow in the ion source reaches the drift tube (Warneke et al., 2001b), which leads to an additional humidification. The measurements were done at an E/N of approximately 120 Td. Acetone and toluene were supplied from a calibration gas, and the mixing ratio was kept constant during the

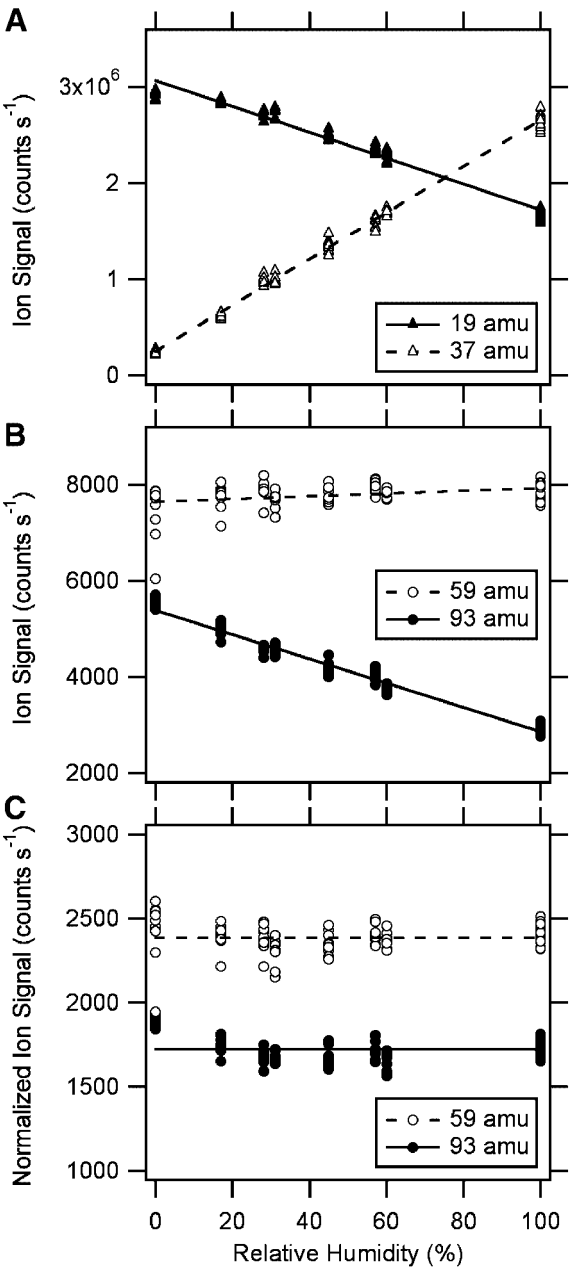

FIGURE 6. Effect of humidity on the detection of acetone at 59 amu and toluene at 93 amu. The experiment was done at 298 K.

experiment. Figure 6A shows the dependence of H_3O^+ and $H_3O^+(H_2O)$ on the relative humidity. It can be seen that the sum of the H_3O^+ and $H_3O^+(H_2O)$ signals goes up with the humidity: $H_3O^+(H_2O)$ ions are detected with a higher efficiency than H_3O^+ (Steinbacher et al., 2004) and, therefore, as more H_3O^+ ions are converted into $H_3O^+(H_2O)$, the total signal will go up. Figure 6B shows that the acetone signal stays relatively constant with the humidity, whereas the toluene signal goes down by almost a factor of 2. These data demonstrate the importance of studying the sensitivity as a function of humidity.

To account for the effects of humidity, we have adopted a method in which I_{RH^+} is not normalized versus $I_{H_3O^+}$ as in Equation (2.14), but versus $I_{H_3O^+} + X_R \times I_{H_3O^+(H_2O)}$ (de Gouw et al., 2003a). The factors X_R are determined from measurements such as shown in Figure 6 and are different for each VOC (Table 1). X_R accounts for the effects of humidity: when normalized to $I_{H_3O^+} + X_R \times I_{H_3O^+(H_2O)}$, the acetone and toluene signals become independent of the relative humidity (Fig. 6C). Table 1 shows that X_R is around 0.5 for most VOCs. Since the transmission efficiency for $H_3O^+(H_2O)$ is approximately twice as high as for H_3O^+ (Steinbacher et al., 2004), values of X_R around 0.5 can be explained by assuming that the VOCs react with both H_3O^+ and $H_3O^+(H_2O)$ at approximately the same rate. For benzene and toluene, X_R is close to zero, because benzene and toluene react only slowly with $H_3O^+(H_2O)$ (Warneke et al., 2001b). The negative value of X_R for benzene suggests that there is some fragmentation of $H_3O^+(H_2O)$ ions in between the drift tube and the mass spectrometer. It should therefore be noted that the values of X_R depend on the extraction voltages of ions behind the drift tube, and should be measured on a regular basis.

The set-up used for field calibrations is shown in Figure 3. To vary the mixing ratio of VOCs in the inlet air, the flow of calibration gas is kept at a constant value and the inlet flow is varied using the Teflon needle valve at the upstream end of the inlet system. The inlet flow is pumped through the catalyst to remove any VOCs in ambient air. The result of a calibration measurement is shown in Figure 7A. Panel A shows the response of the PTR-MS as a function of the mixing ratio of six VOCs contained in a standard mixture. The measurements have been normalized as discussed in the previous paragraph. It is seen that the response is linear in the mixing ratio, and there are non-zero offsets in the response for methanol, acetaldehyde, and acetone. The sensitivity is determined from the slope of the lines fitted through the data points.

As Equation (2.15) shows, the sensitivity depends on the ion transmission efficiency of the mass spectrometer, which can vary over time, in particular when the electron multiplier ages, and when the ion signals in the system are optimized. Nevertheless, the sensitivity of our PTR-MS system has been highly stable, and

TABLE 1. Measured values of the factor X_R, which is used to correct the measurements for the influence of humidity as described in the text

VOC	X_R
Methanol	0.38
Acetonitrile	0.54
Acetaldehyde	0.48
Acetone	0.58
Benzene	-0.2
Toluene	0.1

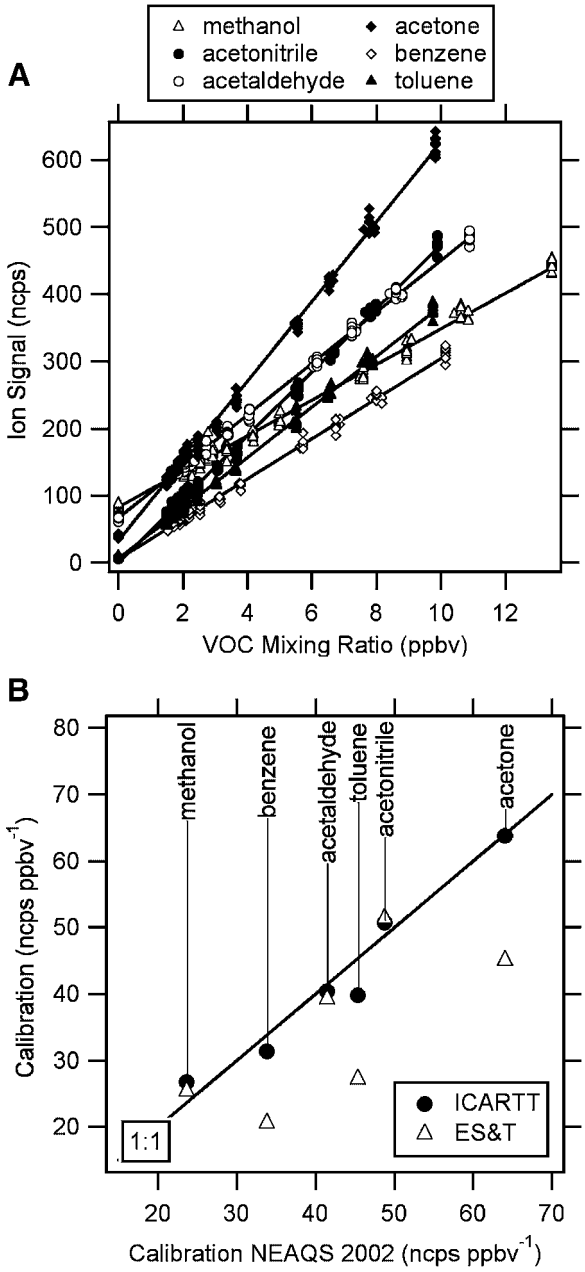

FIGURE 7. **A**: Typical results of a calibration measurement. **B**: Comparison of the calibration factors from the NEAQS 2002 campaign with those from the ICARTT mission (solid circles) and with calculated values published in ES&T (open triangles).

an example is shown in Figure 7B, which compares the calibration factors measured during the ship-based New England Air Quality Study (NEAQS) in 2002 (de Gouw et al., 2003a), with those from aircraft measurements during ICARTT (International Consortium for Atmospheric Research on Transport and Transformation) in 2004 (de Gouw et al., 2006). It is seen that the calibration factors for six VOCs contained in our calibration mixture agree very well between the 2 years. Also shown in Figure 7B are calculated calibration factors published in ES&T (Warneke et al., 2003). The calculation agrees well with the measurement for methanol, acetaldehyde, and acetonitrile. However, the agreement is poor for benzene, toluene, and acetone, which further illustrates why we prefer measured over calculated calibration factors.

3. Detection Limits

The precision of PTR-MS is mostly limited by the counting statistics of the product ions. Several authors have assumed that the counting statistics are Poissonian: the 1σ error in a measurement that is derived from counting a total of N ions is $\sqrt{N}$ (Hayward et al., 2002; de Gouw et al., 2003a). To prove that this assumption is valid, Figure 8 shows the standard deviation (σ) determined from 100 measurements of an ion count N. The agreement between the measured and calculated standard deviation proves (1) that the counting statistics are Poissonian, and (2) that the stability of the ion source is better than 1%, that is, the highest precision obtained in this experiment.

Volume mixing ratios (VMR) are determined from the difference between the count rate of ions detected with the catalyst off ($I_{cc=off}$) and with the catalyst on ($I_{cc=on}$):

$$\mathrm{VMR} = \frac{1}{I_{H_3O^+} \times S}(I_{cc=off} - I_{cc=on}) \qquad (2.16)$$

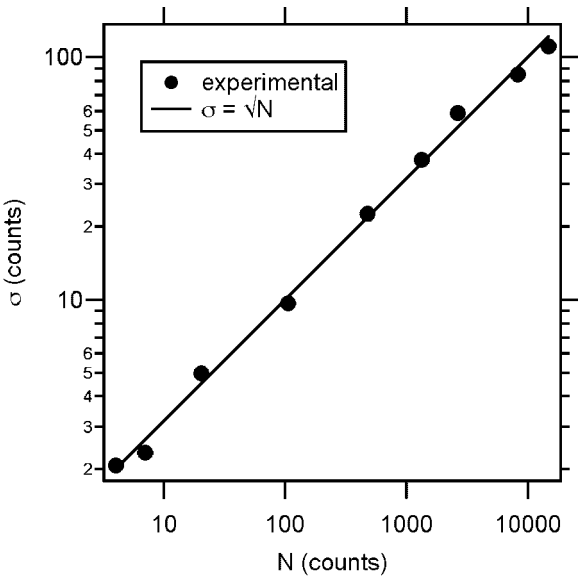

FIGURE 8. Standard deviation (σ) in 100 measurements of an ion count (N) as a function of N. The measured results are compared with the theoretical relationship ($\sigma = \sqrt{N}$) assuming Poissonian counting statistics.

where $I_{H_3O^+}$ is the count rate of H_3O^+ ions (in units of 10^6 counts/sec) and S the calibration factor (in ncps/ppbv). For simplicity the presence of $H_3O^+(H_2O)$ ions is ignored in this equation. From Equation (2.16), the error in the VMR, ΔVMR, can be estimated, assuming that it is dominated by the statistical errors in $I_{cc=off}$ and $I_{cc=on}$ (de Gouw et al., 2003a)

$$\Delta\mathrm{VMR} = \frac{1}{I_{H_3O^+} \times S}\sqrt{\frac{I_{cc=off}}{\tau_{cc=off}} + \frac{I_{cc=on}}{\tau_{cc=on}}} \qquad (2.17)$$

where $\tau_{cc=off}$ and $\tau_{cc=on}$ are the dwell times (in seconds) with the catalyst on and off (not necessarily the same). Equation (2.17) shows that (i) increasing the primary ion signal, (ii) increasing the calibration factor, and (iii) increasing the dwell times will all improve the precision of a measurement. If the VMR is zero, $N_{cc=off} = N_{cc=on}$, and Equation (2.17) can be used to calculate the scatter expected in the PTR-MS measurements. This was verified for isoprene (de Gouw et al., 2003a), and for MEK, benzene, and higher aromatics (de Gouw et al., 2006).

Equations (2.16) and (2.17) describe the precision of a PTR-MS measurement as a function of the VOC mixing ratio. We verified the results in the case of benzene (de Gouw et al., 2003a), and the discussion is summarized here. Figure 9 shows results from an inter-comparison between benzene measurements by PTR-MS and GC-MS during the New England Air Quality Study (NEAQS) in 2002. Figure 9A shows a scatter plot of the PTR-MS versus the GC-MS results and it is seen that the agreement is good with a linear correlation coefficient (r) of 0.93. The solid line shows the result of a best fit to the data, calculated using an orthogonal distance regression (ODR), and has a slope (s) of 1.12 ± 0.08 an intercept (i) of 1 ± 6 pptv. Figure 9B shows the orthogonal residuals between the data and the best fit as a function of the GC measurement. The shaded area shows the scatter in the measurement calculated using Equations (2.16) and (2.17), and describes the distribution of observed residuals very well. Figure 9C shows the relative errors, defined here as the orthogonal residuals divided by the GC measurement, as a function of the GC measurement. Again, the shaded area shows the expected scatter according to Equations (2.16) and (2.17), and it describes the observed scatter very well. Figure 9B shows that the error in the measurement increases gradually as the mixing ratio increases. The relative error, on the other hand, decreases rapidly with the mixing ratio. At very low mixing ratios, the error is >100% and the measurement has no real meaning. One can define the detection limit of the PTR-MS as the mixing ratio where $\Delta\mathrm{VMR}/\mathrm{VMR} = 33\%$ (signal-to-noise = 3). For the example in Figure 9C, we find a detection limit of 35 pptv. This is slightly higher than the detection limit of 32 pptv reported previously (de Gouw et al., 2003a). In that paper, we used the ΔVMR at VMR = 0 to estimate the detection limit. However, Figure 9B shows that ΔVMR increases slightly with VMR, which explains the higher value obtained here.

4. Response Times

The response time of a PTR-MS is determined by a variety of factors. A lower limit is the residence time of sample gas in the drift tube, which varies from 0.2 to 1.0 sec depending on the flow rate and the inner volume of the drift tube. In the earlier designs

the drift tube had a large internal diameter in an effort to establish a homogeneous electric field along the axis of the reactor. In later designs, the internal diameter was smaller to reduce the residence time.

Memory effects further limit the response time of a PTR-MS. It was shown that the PTR-MS signal can linger up to 20 sec after reducing the VOC concentration in the sample flow to zero (Warneke et al., 2003). These memory effects were strongly dependent on the choice of the electrically isolating material in between the drift rings: ketones in particular suffered from strong memory effects when Viton o-rings were used, whereas Teflon and PFA (perfluoro alkoxy) o-rings gave much better results. Karl et al. studied the response time of a PTR-MS coupled to a virtual disjunct eddy covariance inlet system, and found that it was limited more by diffusion effects in the inlet than by memory effects in the drift tube (Karl et al., 2002).

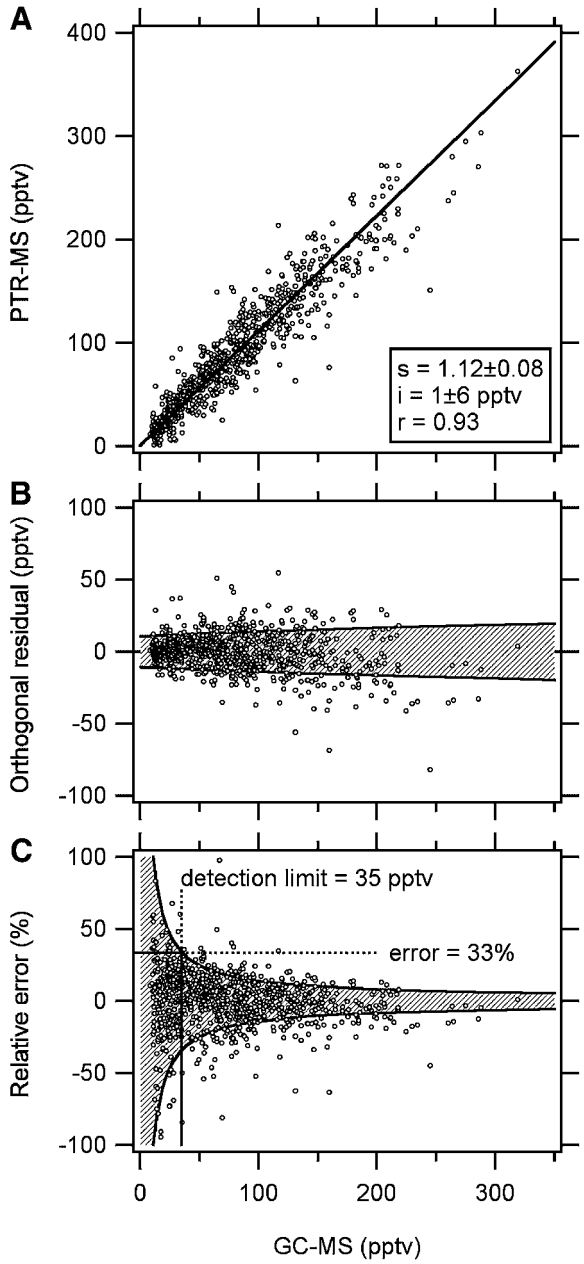

FIGURE 9. Precision of the PTR-MS measurement of benzene during NEAQS 2002. **Panel A** shows a scatter plot of the PTR-MS versus GC-MS results, along with a best fit to the data (solid line). **Panel B** shows the orthogonal residuals between the measurements and the best fit, and **panel C** shows the relative error, defined as the orthogonal residual divided by the GC-MS measurement. The shaded areas in panels B and C show the uncertainties calculated according to Equation (2.16). (GC-MS data are courtesy of Paul Goldan).

III. SPECIFICITY OF PTR-MS

A. GC-PTR-MS

The specificity of PTR-MS has been studied by coupling a gas chromatographic column to the instrument. The column separates the VOCs in a sample prior to the injection into the PTR-MS, which allows the different VOCs that are detected at the same mass to be separated. Of course, this goes at the cost of the rapid response time, but it is a highly valuable tool for studying the specificity of the instrument for individual samples. Karl et al. introduced the method (Karl et al., 2001b,e) and it was further developed in our laboratory to determine the specificity of PTR-MS measurements in urban air (de Gouw et al., 2003b; Warneke et al., 2003).

An example of the result of a GC-PTR-MS analysis of an urban air sample is shown in Figure 10. The figure shows the response of the PTR-MS instrument at eight different masses as a function of the retention time (black lines). The gray areas show the same data, but multiplied by a factor 10 to bring out the smaller peaks. At five out of eight masses, the chromatogram is dominated by one peak, and an on-line PTR-MS measurement at that mass can be attributed with confidence to one specific VOC. At 33 amu, the signal is dominated by methanol, but there is a small peak due to an unknown species at shorter retention times. At 42 amu, there are several small peaks attributed to alkanes, possibly due to O_2^+ reactions, in addition to the main acetonitrile peak (de Gouw et al., 2003c). At 45 amu, a small peak attributed to CO_2 is observed in addition to a peak for acetaldehyde. As CO_2 is not removed by the catalytic converter, one can expect the measurement of acetaldehyde to be corrected for the presence of CO_2. Also, an ethanol peak is observed at 45 amu in more polluted conditions, possibly due to O_2^+ reactions (Spanel & Smith, 1997). At 59 amu, there is a small peak due to propanal in addition to the main peak from acetone. In cleaner conditions the propanal contribution tends to be smaller as it is the more reactive VOC. The signals at 79 and 93 amu are dominated by one peak only, benzene and toluene, respectively. Depending on the value of *E/N* used (these results were obtained at a drift tube pressure of 2.4 mbar and an *E/N* value of 106 Td), higher alkyl benzenes can fragment into ions at 79 amu. These peaks are very small in Figure 10, but larger contributions were seen in measurements at the Sonnblick Observatory with a different instrument (de Gouw et al., 2003b). The signals at 107 and 121 amu show the presence of several isomers of C_8- and C_9-aromatics, respectively. These isomers

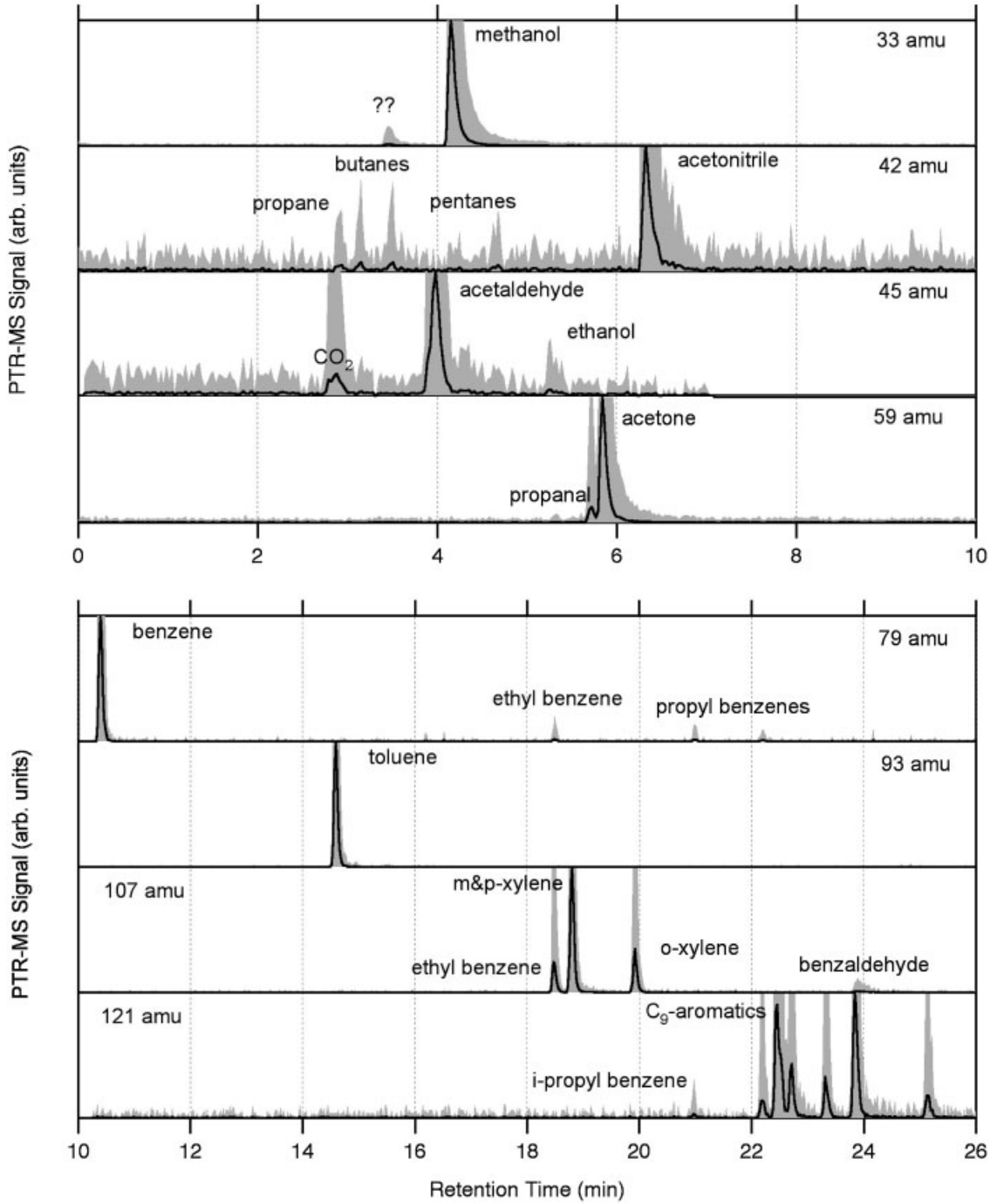

FIGURE 10. Example of a GC-PTR-MS analysis of an urban air sample. Sample was collected in Boulder, Colorado, in January 2002. The black lines show the signals at various masses. The shaded areas show the same signals, but multiplied by 10 to bring out the smaller scale features.

cannot be separately measured using PTR-MS, but one can expect the measurement at 107 and 121 amu to be equivalent to a sum measurement. At 107 amu, there is a very small additional peak attributed to benzaldehyde.

GC-PTR-MS analyses are highly valuable in determining which species contribute to the signal at a certain mass. So far, GC-PTR-MS has been used to analyze certain types of biogenic emissions (Karl et al., 2001b,e) and winter-time, urban air (de Gouw et al., 2003b; Warneke et al., 2003). More work can and should be done to study the specificity of PTR-MS in other types of air masses, for example biomass burning emissions, and biogenic emissions from different ecosystems.

B. Inter-Comparisons

Detailed inter-comparisons between PTR-MS and alternative methods for VOC measurements have been published elsewhere (de Gouw et al., 2003a; Kuster et al., 2004), and show generally good agreement with some notable exceptions. Here, we will first discuss some further results obtained during the ICARTT (International Consortium for Atmospheric Research on Transport and Transformation) study in 2004. We will then summarize the published inter-comparisons and draw some general conclusions.

1. VOC Inter-Comparison During ICARTT

The ICARTT collaboration involved an air quality study in the northeastern United States as well as a long-range transport study of North American pollution across the Atlantic Ocean (Brown et al., 2005; de Gouw et al., 2006; Warneke et al., 2006). The study involved airborne measurements with the NOAA WP-3D research aircraft in the northeastern US and provided another opportunity to inter-compare PTR-MS with an alternative technique, in this case GC analyses of whole air samples (WAS). Figure 11 shows scatter plots of the PTR-MS versus the

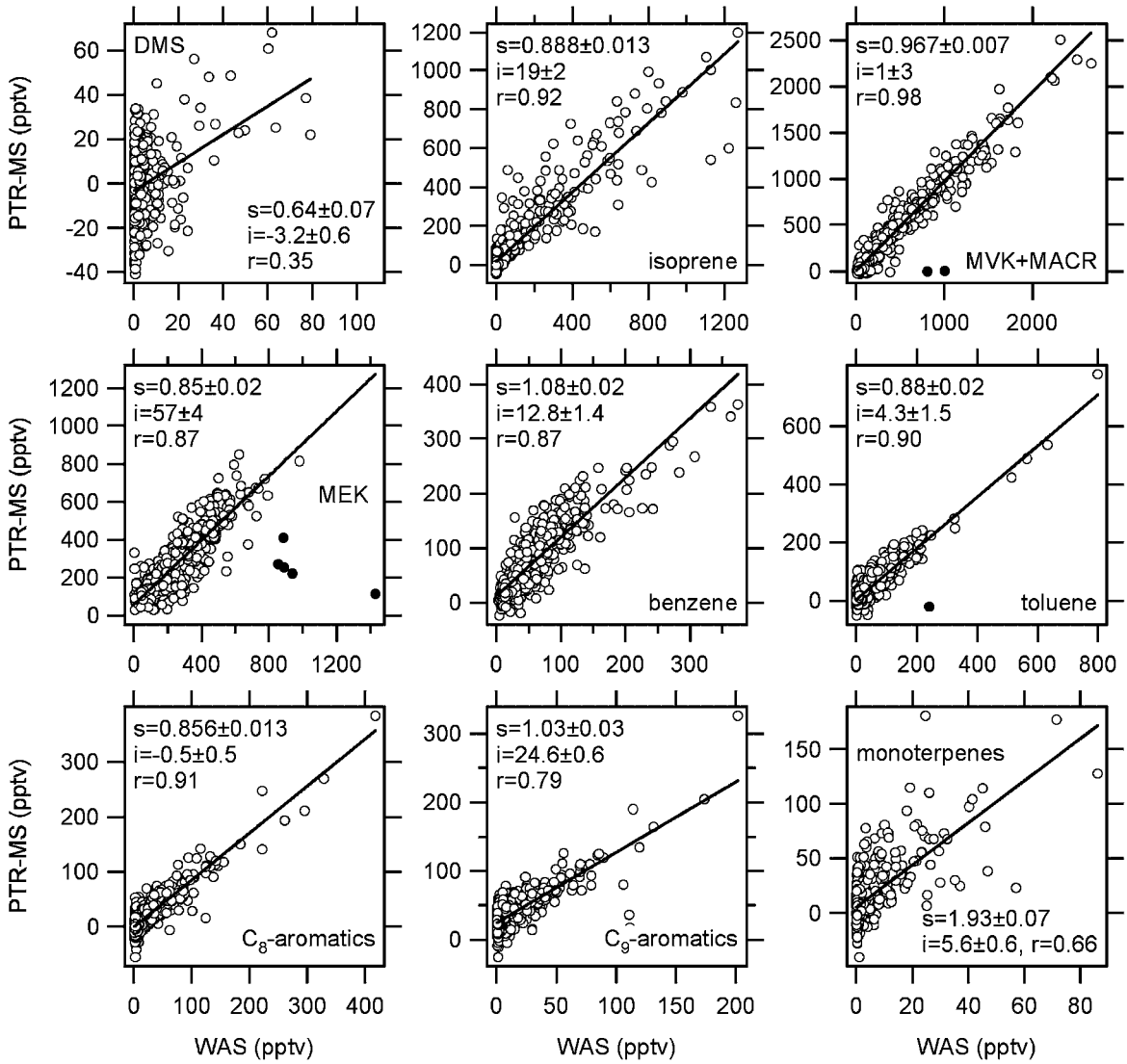

FIGURE 11. Inter-comparison between airborne VOC measurements by PTR-MS and by GC analyses of whole air samples (WAS) during the ICARTT study. The open circles show the measured data, and the solid lines the best linear fits to the data. The solid circles show several outliers that are discussed in the text. Also given are the slopes (s) and intercepts (*i*, in units of pptv) derived from the fits, and the linear correlation coefficient (*r*). (WAS data are courtesy of Elliot Atlas).

WAS results from all research flights. Data are included for all species that were quantified by both methods. The PTR-MS data were interpolated on the time basis of the WAS measurements for the purpose of this comparison. The inter-comparison results for MEK and the aromatics have been presented elsewhere (de Gouw et al., 2006); the results for DMS, isoprene, MVK + MACR, and the monoterpenes are presented here for the first time.

The PTR-MS and WAS for all species except DMS and the monoterpenes agree within a 15% calibration uncertainty and with relatively high linear correlation coefficients (r), ranging from 0.79 for the C_9-aromatics to 0.98 for the sum of methyl vinyl ketone and methacrolein (MVK + MACR). For several species (MVK + MACR, MEK, and toluene) there are a few outliers in the scatter plots, for which an elevated WAS measurement was not observed by the PTR-MS (solid circles in Fig. 11). In all cases we suspect human error to be the cause for the outliers, which is not uncommon when working with these large data sets. The outliers were omitted in calculating best fits for the scatter plots, and the slopes and intercepts are given in Figure 11. In the case of DMS and the monoterpenes the agreement between PTR-MS and WAS was much poorer than for the other species, and these measurements are discussed in more detail below. Finally, it should be mentioned that massive but aged forest fire plumes were encountered during ICARTT (de Gouw et al., 2006); the data points obtained in these plumes did not deviate from the general trends observed in Figure 11.

One problem in the measurement of DMS is interference from $H^+(CH_3CHO)(H_2O)$ clusters. This problem is illustrated in Figure 12, which shows a scatter plot of the DMS versus acetaldehyde signal for all the data collected onboard the NOAA WP-3D aircraft during the ICARTT study. The figure shows that with increasing acetaldehyde, the lowest measured DMS mixing ratio also increases. We attribute this to interference from $H^+(CH_3CHO)(H_2O)$ clusters. There are also some points with enhanced DMS at low acetaldehyde mixing ratios, which we attribute to the presence of DMS. The solid line in Figure 12 shows the estimated contribution from $H^+(CH_3CHO)(H_2O)$ ions to the DMS results, and has a slope of 0.036 pptv/pptv. In other words the sensitivity for DMS is ~28 times higher than that for acetaldehyde at 63 amu, but it is a problem since acetaldehyde is typically much higher in the atmosphere than DMS. The DMS data in Figure 11 have been corrected for this effect, but the scatter plot still shows a poor correlation with the WAS measurements. Part of the reason is that only very few air masses with elevated DMS were encountered with the aircraft. As a result, the scatter plot in Figure 11 is dominated by statistical noise and does not do full justice to the inter-comparison of the results. Figure 13, for example, shows results from the flight on July 25, when the highest DMS was measured. The flight track is shown in Figure 13A and shows elevated DMS (1) over southeastern Massachusetts, (2) just south of Long Island, and (3) just off the coast of New Jersey. All three features are captured by both measurements (Fig. 13B), but there are only 4 WAS measurements above 40 pptv and they hardly impact the scatter plot in Figure 11.

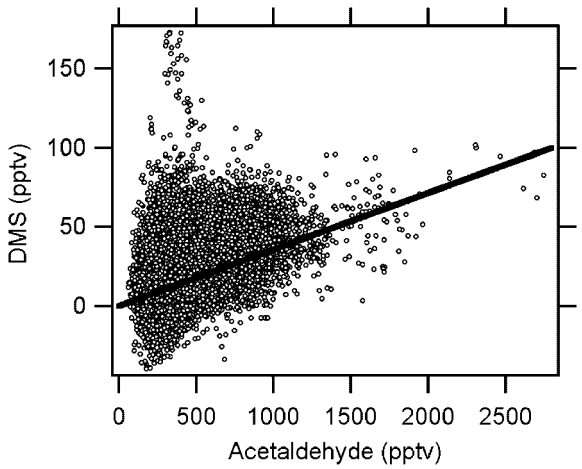

FIGURE 12. Scatter plot of mass 63 (DMS) versus mass 45 (acetaldehyde) data from airborne measurements onboard the NOAA WP-3D during the ICARTT study. The black line shows the estimated contribution from $H^+(CH_3CHO)(H_2O)$ ions to the signal at 63 amu, which is used to quantify DMS.

The correlation between the PTR-MS and WAS measurements of monoterpenes was reasonable ($r = 0.66$), but the quantitative agreement was poor with a slope of 1.93 ± 0.07 pptv/pptv derived from the scatter plot (Fig. 11). It should be noted that only α- and β-pinene from the WAS measurements were added for the comparison, whereas previous work has shown that other monoterpenes also contribute significantly to the PTR-MS signal (de Gouw et al., 2003a). Nevertheless, the total contribution of α- and β-pinene varied between 60% and 80% in the NEAQS 2002 data (de Gouw et al., 2003a), and the omission of other species in the present study can probably not account for the difference between PTR-MS and WAS. As in the case of DMS, a scatter plot does only partial justice to the inter-comparison. When comparing a species with an extremely short atmospheric lifetime such as isoprene or the monoterpenes, the exact timing between the two different measurements becomes important. In the present case, there can be as much as 20 sec between the PTR-MS and WAS measurements, and this contributes to some of the scatter observed in Figure 11. Figure 14 shows results from the flight on July 22, when the highest monoterpenes were measured. The flight track in Figure 14A shows elevated monoterpenes over Nova Scotia and Maine, and much lower values over the ocean as expected. Figure 14B–D show the time series of the PTR-MS and WAS measurements of isoprene, MVK + MACR, and the monoterpenes, respectively, and the agreement is quite good. The WAS measurements of monoterpenes have been multiplied by a factor of 2 for the purpose of this plot, and also show a good agreement although later in the flight, around 8:00–9:00 pm UTC when the photochemical activity was high, the PTR-MS measurement seems to be systematically higher.

2. *Summary of Published Work*

Table 2 summarizes the inter-comparisons between PTR-MS and alternative methods that have been published. It is seen that with a few exceptions, most of the slopes of the scatter plots (PTR-MS vs. alternative method) are equal to 1 within 20%, which is a good estimate of the measurement accuracy. In case of the

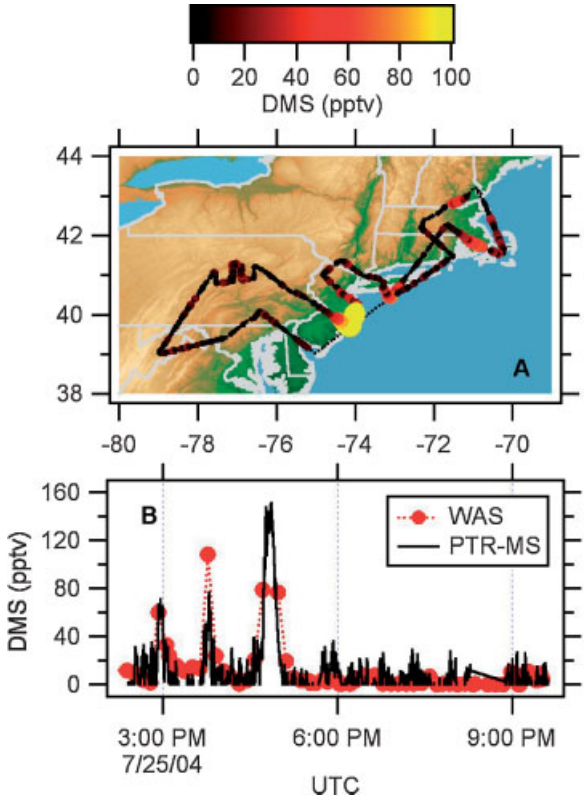

FIGURE 13. **A**: Flight track of the NOAA WP-3D on July 25, 2004, color-coded by the DMS mixing ratio measured by PTR-MS. **B**: Inter-comparison between the PTR-MS and WAS measurements of DMS. (WAS data are courtesy of Elliot Atlas).

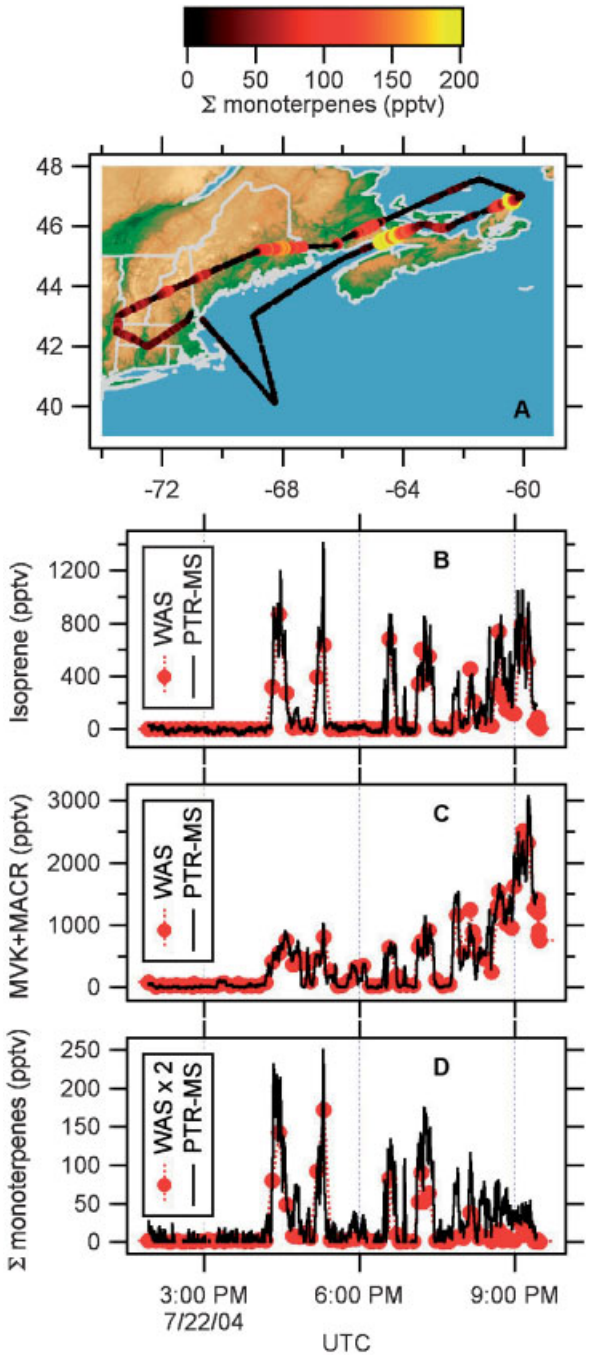

FIGURE 14. **A**: Flight track of the NOAA WP-3D on July 22, 2004, color-coded by the monoterpene mixing ratio measured by PTR-MS. **B**–**D**: Inter-comparison between the PTR-MS and WAS measurements of (B) isoprene, (C) MVK + MACR and (D) monoterpenes. (WAS data are courtesy of Elliot Atlas).

monoterpenes and the C_8- and C_9-aromatics, the PTR-MS measurement is compared with the sum of multiple species, and the combined uncertainties are somewhat higher.

Figure 15 shows histograms of the slopes and intercepts reported in Table 2. The full curves show the result of fitting a Gaussian distribution to these histograms. The distribution of the slopes is centered on 0.91 pptv/pptv with a width of 0.20 pptv/pptv, that is, equal to 1 within the 1σ scatter of the individual results. The outliers in Figure 15A (slope >2 pptv/pptv) include the C_9-aromatics (Kuster et al., 2004), isoprene (Kato et al., 2004), MEK, and the C_8-aromatics (de Gouw et al., 2003a). In all of these cases, the other published inter-comparisons agree much better (Table 2), so the differences are not necessarily systematic. We conclude that the average accuracy of the published PTR-MS measurements is limited to approximately 20%. The distribution of the intercepts is centered on 2.8 pptv with a width of 12 pptv, that is, equal to 0 within the 1σ scatter of the individual results. This may suggest that there are no significant biases in PTR-MS. However, the distribution in Figure 15B is skewed: 34 of 51 studies gave positive intercepts. The outliers in Figure 15B with negative intercepts >100 pptv include methanol (de Gouw et al., 2003a, 2004b), acetaldehyde (de Gouw et al., 2003a), and acetone (de Gouw et al., 2004b), and with positive intercepts >100 pptv include propylene (Kuster et al., 2004), isoprene (Kato et al., 2004; Kuster et al., 2004), benzene (Warneke et al., 2001b), toluene (Kato et al., 2004), and the C_8-aromatics (Steinbacher et al., 2004). The negative intercepts for oxygenated species may be attributable to the fact that the PTR-MS measurements are corrected for backgrounds of such species in the instrument. The positive intercepts for the hydrocarbons are most likely due to interferences from different VOCs at low

TABLE 2. Published inter-comparisons between PTR-MS and alternative methods

VOC	Mass (amu)	Reference	Other method	Slope	Intercept (pptv)
Formaldehyde	31	(Steinbacher et al., 2004)	Hantzsch	N/A	
Methanol	33	(de Gouw et al., 2003a)	on-line GC-MS	1.028	-110
		(de Gouw et al., 2004b)	PTR-MS	1.16	-170
Acetonitrile	42	(Sprung et al., 2001)	AP-CIMS	0.86	40
		(de Gouw et al., 2003a)	on-line GC-MS	0.91	-3
		(de Gouw et al., 2004b)	PTR-MS	1.03	-16
Propylene	43	(Kuster et al., 2004)	on-line GC-FID	0.9	2700
Acetaldehyde	45	(Kuster et al., 2004)	on-line GC-ITMS	N/A	
		(de Gouw et al., 2003a)	on-line GC-MS	1.56	-170
Acetone	59	(Sprung et al., 2001)	AP-CIMS	1.18	63
		(Kuster et al., 2004)	on-line GC-ITMS	0.95	0
		(de Gouw et al., 2003a)	on-line GC-MS	1.002	-50
		(de Gouw et al., 2004b)	PTR-MS	1.05	-200
		(Ammann et al., 2004)	on-line GC-FID	N/A	
DMS	63	This work	GC canisters	0.64	-3.2
Isoprene	69	(de Gouw et al., 2003a)	on-line GC-MS	0.97	14
		(Kuster et al., 2004)	on-line GC-ITMS	1.1	100
		(Kuster et al., 2004)	on-line GC-FID	1.2	100
		(Kuster et al., 2004)	on-line GC-QMS	0.96	120
		(Ammann et al., 2004)	on-line GC-FID	N/A	
		(Kato et al., 2004)	on-line GC-FID	2.15	212
		This work	GC canisters	0.888	19
MVK+MACR	71	(de Gouw et al., 2003a)	on-line GC-MS	1.01	6
		(Ammann et al., 2004)	on-line GC-FID	N/A	
		This work	GC canisters	0.967	1
MEK	73	(de Gouw et al., 2003a)	on-line GC-MS	2.51	16
		(de Gouw et al., 2006)	GC canisters	0.85	57
PAN	77	(de Gouw et al., 2003a)	GC-ECD	0.72	60
Benzene	79	(Warneke et al., 2001b)	GC canisters	0.82	106
		(Kuster et al., 2004)	on-line GC-ITMS	0.85	0
		(Kuster et al., 2004)	on-line GC-QMS	0.91	0
		(de Gouw et al., 2003a)	on-line GC-MS	1.12	1
		(de Gouw et al., 2004a)	GC canisters	1.04	15
		(Ammann et al., 2004)	on-line GC-FID	N/A	
		(Kato et al., 2004)	on-line GC-FID	0.82	26
		(de Gouw et al., 2006)	GC canisters	1.08	12.8
Toluene	93	(Warneke et al., 2001b)	GC canisters	1.18	-66
		(Kuster et al., 2004)	on-line GC-ITMS	0.97	0
		(Kuster et al., 2004)	on-line GC-QMS	0.81	100
		(de Gouw et al., 2003a)	on-line GC-MS	1.08	10
		(de Gouw et al., 2004a)	GC canisters	0.83	23
		(Kato et al., 2004)	on-line GC-FID	0.52	158
		(de Gouw et al., 2006)	GC canisters	0.88	4.3
Styrene	105	(Kuster et al., 2004)	on-line GC-ITMS	0.9	40
C_8-aromatics	107	(Kuster et al., 2004)	on-line GC-ITMS	1.02	0
		(de Gouw et al., 2003a)	on-line GC-MS	3.2	11
		(Steinbacher et al., 2004)	GC filters	0.78 [a]	150
		(Kato et al., 2004)	on-line GC-FID	0.58	0.7
		(de Gouw et al., 2006)	GC canisters	0.856	-0.5
C_9-aromatics	121	(Kuster et al., 2004)	on-line GC-ITMS	2.01	0
		(de Gouw et al., 2003a)	on-line GC-MS	1.35	33
		(Kato et al., 2004)	on-line GC-FID	0.98	93
		(de Gouw et al., 2006)	GC canisters	1.03	24.6
Monoterpenes	137	(de Gouw et al., 2003a)	on-line GC-MS	0.80	19
		(Kato et al., 2004)	on-line GC-FID	0.96	33
		(Lee et al., 2005)	GC-FID bags	1.30	0
		This work	GC canisters	1.93	5.6

[a]These authors reported significant discrepancies during the summer months.

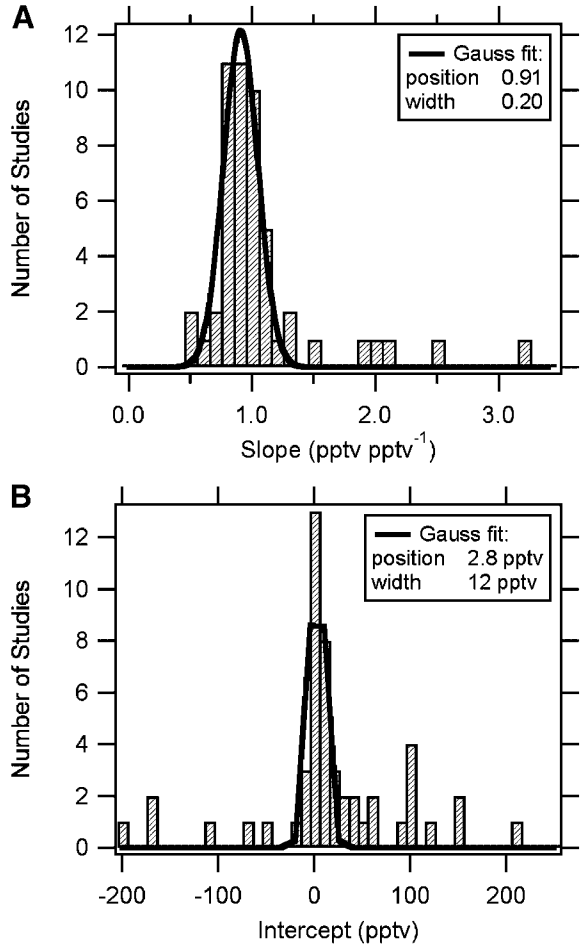

FIGURE 15. Histograms of (**A**) the slopes and (**B**) the intercepts determined from the inter-comparison studies given in Table 2.

levels. Particularly, the measurements of propylene and to a lesser extent isoprene are problematic at low levels. The results of the inter-comparisons summarized in Table 2 are discussed for each species in the next section.

Most of the inter-comparisons have been performed in urban air, forest air, or the free troposphere. Much less work has been done on biomass burning plumes in the atmosphere, whereas direct emissions measurements have indicated that the compound identification for some masses could show some marked differences (Christian et al., 2004).

C. Detection of Different VOCs by PTR-MS

The findings from the GC-PTR-MS and the inter-comparison studies are discussed in this section for each VOC.

1. Mass 31: Formaldehyde

Formaldehyde is a difficult compound to detect by PTR-MS: the proton affinity is only slightly higher than that of water, and as a result the back-reaction between protonated formaldehyde and water is not negligible. Because of the back-reactions, the sensitivity is low and, moreover, humidity dependent. The kinetics of the forward- and back-reactions were measured (Hansel et al., 1997), and the results can be used to calculate the response of the PTR-MS for formaldehyde. A direct calibration of the PTR-MS for this compound has not been published. A comparison between formaldehyde measurements by PTR-MS and the Hantzsch method has been presented (Steinbacher et al., 2004), but the correlation between the two measurements was not very good. More work is needed (1) to characterize the response of PTR-MS for formaldehyde as a function of humidity, and (2) to verify that no other species are detected at 31 amu.

2. Mass 33: Methanol

GC-PTR-MS measurements have not shown a significant presence of species other than methanol at 33 amu. Two inter-comparisons were reported (Table 2). Both studies showed slopes that were equal to 1 within 20%, but significant intercepts in the alternative method. These intercepts are somewhat uncertain, since in most air masses the methanol mixing ratios are significantly higher than the intercepts. Calibrations for methanol are difficult as it interacts strongly with metal surfaces, for example, in pressure reducers and flow controllers, and it can take up to several days until the amount of methanol in a diluted calibration standard becomes stable (de Gouw et al., 2003a).

3. Mass 42: Acetonitrile

GC-PTR-MS measurements have indicated that small alkanes can be detected at 42 amu as a result of the reactions with O_2^+ ions. However, the sensitivity for the alkanes is relatively small, and does not interfere strongly with the detection of acetonitrile. The inter-comparisons in Table 2 all show slopes equal to 1 within 20%. There was an intercept of around 40 pptv in the comparison with AP-CIMS (Sprung et al., 2001), which is a significant fraction of the ambient mixing ratio.

4. Mass 43: Multiple Species

Multiple species are detected at 43 amu in PTR-MS, and the measurement is not unique for any of them. An inter-comparison between propylene measurements in Houston, Texas, by PTR-MS and an on-line GC-FID method has been published (Kuster et al., 2004). Houston has unusually high emissions of propylene as a result of the presence of numerous petrochemical industries. In pollution plumes with many ppbv of propylene, the agreement between PTR-MS and GC-FID was reasonable, but the inter-comparison revealed an offset in the PTR-MS measurement of 2.7 ppbv due to interfering species such as, most likely, acetone, acetic acid, PAN propanol and several hydrocarbons. As propylene is much lower than 2.7 ppbv in most air masses, the PTR-MS instrument cannot be used to measure propylene. It may be possible to subtract the interfering contributions of acetone, acetic acid and PAN, which are also detected at other masses, but this is yet to be proven, and the resulting propylene measurement will not have a very high precision.

5. Mass 45: Acetaldehyde

Atmospheric measurements of acetaldehyde have shown mixing ratios of 100–200 pptv in the background troposphere, and these results are difficult to explain with our current understanding of the sources and photochemistry of acetaldehyde (Singh et al., 2001, 2003). Multiple groups, however, have reported the potential of measurement artifacts (Apel et al., 2003; Northway et al., 2004), and for these reasons the PTR-MS measurement of acetaldehyde is discussed in somewhat more detail in this paper.

As shown in Figure 10, GC-PTR-MS analyses have shown that a PTR-MS measurement at 45 amu is dominated by acetaldehyde. A minor peak is attributed to CO_2 and should be corrected by the subtraction of the background signal measured with the catalytic converter. In polluted conditions, a minor peak attributed to ethanol is observed in the chromatograms, possibly from the reactions with O_2^+ (Spanel & Smith, 1997). Nevertheless, the ethanol peak is always much smaller than the acetaldehyde peak, and not observed in clean conditions. Several other small peaks were observed at the Sonnblick Observatory in air masses that were heavily influenced by biogenic emissions (de Gouw et al., 2003b). These peaks have not been observed in urban air samples.

It should be noted that the GC-PTR-MS measurement does not allow measurements of species that (i) cannot be collected in the cryo-cooled sample trap, (ii) dissociate as a result of the heating during the injection, or (iii) are not separated by the column used. As a result of these limitations, it is possible that a GC-PTR-MS analysis only shows the presence of one VOC, whereas other species are detected at that mass in an on-line PTR-MS measurement. To study this possibility, the results of GC-PTR-MS measurements were compared quantitatively with those from on-line PTR-MS measurements (Warneke et al., 2003), and revealed no problems for acetaldehyde.

Only one inter-comparison of PTR-MS with an independent alternative method, on-line GC-MS, has been reported (de Gouw et al., 2003a). The correlation between the two measurements was good with a linear correlation coefficient, r, of 0.86. However, the quantitative agreement was not good: the slope of the scatter plot of PTR-MS versus GC-MS was 1.56 ± 0.04. The difference was attributed to inaccuracies in the calibration gases used, and there is some later evidence that this was indeed the case: both a GC-PTR-MS study (Warneke et al., 2003) and an inter-comparison between GC-MS and PIT-MS, a new technique based on the same ion chemistry (a PTR-MS with an ion trap mass spectrometer) (Warneke et al., 2005b), gave a better quantitative agreement for acetaldehyde. PIT-MS is discussed further below in Section V. In the clean, marine boundary layer both PTR-MS and GC-MS showed the presence of more than 100 pptv of acetaldehyde.

Both on the DLR Falcon and NOAA WP-3D research aircraft, a PTR-MS was used to sample a stratospheric intrusion and in both cases the same was observed. As one would expect, most VOCs were anti-correlated with ozone; however, acetaldehyde was positively correlated with ozone (Fig. 16). The intrusion over the Mediterranean from the Falcon has been described elsewhere (Fischer et al., 2003), and Figure 16 shows the acetaldehyde data from this event. A surprisingly similar relationship between acetaldehyde and ozone was observed from

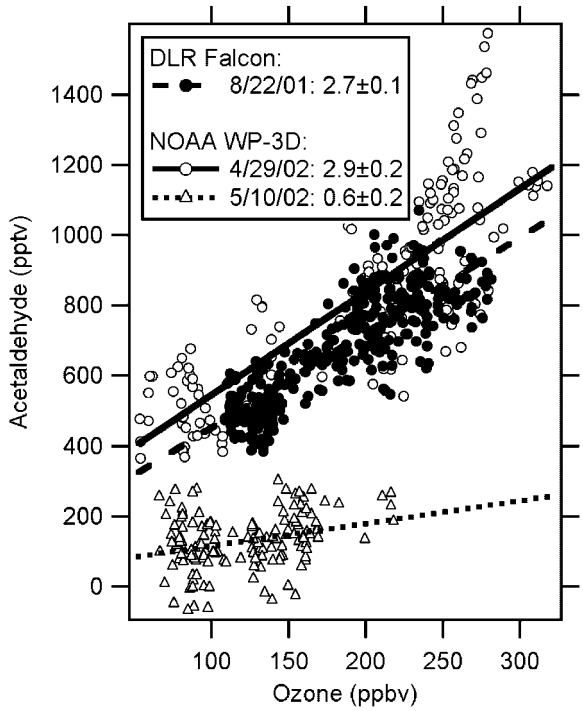

FIGURE 16. Scatter plots of acetaldehyde versus ozone inside stratospheric intrusions from different flights onboard the DLR Falcon and NOAA WP-3D research aircraft. The solid lines are linear fits to the data, and the slopes are indicated in the legend. (Ozone data from the DLR Falcon are courtesy of Hans Schlager; ozone data from the WP-3D are courtesy of John Holloway).

the NOAA WP-3D in an intrusion over the Pacific Ocean (Northway et al., 2004). However, positive correlations between acetaldehyde and ozone are not always observed, as the data from May 10, 2002, in Figure 16 show. At this point we think that the positive correlation between acetaldehyde and ozone in stratospheric intrusions is most likely an artifact of the measurement. Ozone may react with impurities on the surface of the inlet system, with acetaldehyde as a product (Northway et al., 2004). It would be a surprisingly efficient mechanism to generate acetaldehyde, however. Because our inlet is similar to an inlet used for an ozone measurement, it can be expected that most of the ozone does not react at the surface of the inlet. If we assume an actual ozone loss of 1%–2%, the reaction forms acetaldehyde with a yield of 15%–30%, considering the observed acetaldehyde-to-ozone slopes of ~3 pptv/ppbv (Fig. 16). Such high yields are hardly observed in case of pure liquids that are known to produce acetaldehyde in reaction with ozone (Northway et al., 2004), and are therefore surprisingly high for random impurities.

It is not certain that similar acetaldehyde artifacts exist when sampling tropospheric air. Several findings argue against that possibility: (i) strong correlations between acetaldehyde and ozone have not been observed in the troposphere (de Gouw et al., 2003a), and (ii) it has been difficult to reproduce the production of acetaldehyde from ozone in dirty inlets in the laboratory (Northway et al., 2004). However, if similar artifacts do exist when sampling tropospheric air, then the background levels of acetaldehyde in the troposphere are highly suspect: assuming an

acetaldehyde-to-ozone slope of ~3 pptv/ppbv (Fig. 16), a typical tropospheric ozone level of 60 ppbv would generate 180 pptv of acetaldehyde, which is in the range of background levels observed by us and others (Singh et al., 2001, 2003). It should also be noted that an ozone artifact might not be limited to PTR-MS measurements, if it involves the reaction of ozone with an inlet system. Indeed, the acetaldehyde-to-ozone slope of ~3 pptv/ppbv observed here is very similar to that reported for laboratory tests with a GC-MS system (Apel et al., 2003).

In summary, we believe that the measurement of acetaldehyde in polluted air is most likely without problems. However, the 100–200 pptv background levels of acetaldehyde in the troposphere should be regarded with suspicion. Since acetaldehyde is such a reactive trace gas, resolving these issues is important and should receive a lot of attention.

6. Mass 59: Acetone

Acetone and propanal are both detected at 59 amu in PTR-MS, but multiple studies have shown that the contribution from propanal is typically only small (0%–10%), and for practical purposes the measurement at 59 amu can be regarded as a measurement of acetone. Four inter-comparisons are included in Table 2 and the slopes were all equal to 1 within 20%. As in the case of methanol, there can be significant intercepts in the alternative method, which are uncertain as acetone mixing ratios in the atmosphere are typically much higher than the intercepts.

7. Mass 61: Acetic Acid

Acetic acid is detected at 61 amu in PTR-MS. The signal at 61 amu has been shown to correlate well with the results of acetic acid measurements by mist-chamber sampling and ion chromatography analyses (de Gouw et al., 2003a). The response of PTR-MS for acetic acid has not been properly calibrated due to the difficulty to produce reliable gas-phase standards. The need for calibrations is all the more important, however, since memory effects of acetic acid in the inlet system and/or drift tube reactor have been inferred from the measurements (de Gouw et al., 2003a, 2006). More work is necessary to determine the validity of acetic acid measurements by PTR-MS. Nevertheless, there are good indications that reliable measurements are possible.

8. Mass 63: Dimethyl Sulfide (DMS)

No GC-PTR-MS or inter-comparison studies have been reported for DMS other than the work in this paper. The measurement of DMS suffered from interference from acetaldehyde clusters (Fig. 12), and after correction for this effect, a reasonable agreement with GC measurements was obtained in relatively clean marine air masses (Fig. 13). Averaged over larger regions of the atmosphere, the agreement between PTR-MS and GC was poor (Fig. 11). Recent work using a novel PIT-MS instrument has shown good agreement between measurements of DMS with a GC-MS and with a PIT-MS using the signal at 63 amu (Warneke et al., 2005b). More work is needed to study the magnitude of the acetaldehyde interference as a function of humidity and *E*/*N*: it can be expected that the problem is less severe at higher *E*/*N*.

9. Mass 69: Isoprene

Isoprene measurements by PTR-MS, at 69 amu, have been inter-compared in multiple studies. In five out of six cases, the agreement was within 20% (Table 2). Atmospheric measurements of isoprene away from biogenic sources should be regarded with some caution: GC-PTR-MS analyses have shown that multiple (biogenic) species can contribute to the measurement at 69 amu, including 2- and 3-methyl butanal and 1-penten-3-ol (Karl et al., 2001b,e). Also, multiple unidentified species were observed in GC-PTR-MS analyses of urban air (de Gouw et al., 2003b). A VOC emitted from certain pine trees, 2-methyl-3-buten-2-ol or MBO, is also detected at 69 amu, and interferes with the detection of isoprene in those regions where MBO emissions from vegetation are significant (Holzinger et al., 2005a). Finally, in biomass burning plumes a large contribution to the signal at 69 amu is almost certainly from furan (Christian et al., 2004).

Despite the presence of multiple interferences, PTR-MS measurements of isoprene have compared well versus alternative techniques in a variety of conditions, including those impacted by industrial emissions (Kuster et al., 2004), fresh and aged urban emissions (de Gouw et al., 2003a), and aged forest fire emissions (Fig. 11). Evidently, the natural sources of isoprene overwhelm those of its interferences in many regions of the atmosphere.

10. Mass 71: Methyl Vinyl Ketone + Methacrolein (MVK + MACR)

Methyl vinyl ketone and methacrolein are products from the atmospheric oxidation of isoprene, and both are detected at 71 amu. They cannot be separately measured by PTR-MS, but inter-comparisons have shown that the PTR-MS measurement can be regarded as a sum measurement (Table 2). No GC-PTR-MS analyses for mass 71 have been published. As in the case of isoprene, PTR-MS measurements of MVK and MACR have compared well versus alternative techniques in a variety of conditions, including those impacted by fresh and aged urban emissions (de Gouw et al., 2003a), and aged forest fire emissions (Fig. 11).

11. Mass 73: Methyl Ethyl Ketone (MEK)

Methyl ethyl ketone is detected at 73 amu in PTR-MS. Its measurement is complicated by the presence of $H_3O^+(H_2O)_3$ cluster ions at that mass, the concentration of which is strongly humidity dependent (Fig. 4C). Two inter-comparisons have been published (Table 2). An inter-comparison with an on-line GC-MS measurement gave a good correlation but a poor quantitative agreement (de Gouw et al., 2003a). The difference was attributed to calibration uncertainties. A recent inter-comparison with GC analyses of air samples gave a much better, quantitative agreement (de Gouw et al., 2006) (Fig. 11). As a result of the background from $H_3O^+(H_2O)_3$, the precision of the measurement is somewhat reduced. No GC-PTR-MS work has been reported to address potential interferences, for example, from butanal, detected at the same mass.

12. Mass 77: Peroxyacetyl Nitrate (PAN)

Laboratory work and field tests indicated that different peroxyacyl nitrate compounds (PANs) can be detected by PTR-MS (Hansel & Wisthaler, 2000). Onboard the NOAA research ship Ronald H. Brown in 2002, the PTR-MS signal at 77 amu was found to correlate extremely well with a PAN measurement by GC-ECD, and after calibrating the PTR-MS the two results were found to agree within 30% (de Gouw et al., 2003a). Using almost the exact same set-up it was found in 2004, however, that the PTR-MS signal at 77 amu suffered from interference due to $H_3O^+(CH_3COCH_3)$ cluster ions, which is dependent on the ambient mixing ratio of acetone, that is, a markedly different behavior from the observations in 2002. The detection of PAN and interference from acetone is evidently more sensitive to the operating conditions of the PTR-MS than previously recognized, and more detailed laboratory work is necessary to determine the exact operating conditions required.

13. Mass 79: Benzene

Benzene is detected at 79 amu in PTR-MS, and its measurement has been inter-compared many times with mostly favorable results (Table 2). Its measurement can be slightly humidity dependent (Warneke et al., 2001b), similarly to toluene (Fig. 6). Most likely this effect is less pronounced at higher values of *E/N*, since in that case the reagent ions are dominated by H_3O^+. However, a disadvantage of working at a higher *E/N* value is that higher aromatics can start to fragment into ions at 79 amu, as demonstrated for ethyl and propyl benzene (Fig. 10) (de Gouw et al., 2003b).

14. Mass 93: Toluene

Toluene is detected at 93 amu in PTR-MS and has been inter-compared many times versus alternative methods with mostly favorable results (Table 2). As demonstrated in Figure 6, its measurement is slightly humidity dependent. A minor interference comes from monoterpenes, which can fragment into ions at 93 amu (Warneke et al., 2003). However, even in air masses with strongly enhanced monoterpene, but low toluene concentrations, this interference is not readily apparent from the data (de Gouw et al., 2003a).

15. Mass 105: Styrene and Peroxy Isobutyryl Nitrate (PiBN)

Styrene is detected at 105 amu in PTR-MS, and a published inter-comparison between PTR-MS and an on-line GC-ITMS showed a good agreement (Table 2). This study was performed in Houston, Texas, where styrene emissions from the petrochemical industry are large (Kuster et al., 2004). In most regions, the mixing ratios of styrene will not be that high, and it was found that peroxy isobutyryl nitrate (PiBN), an atmospheric oxidation product from iso-butane, also contributes significantly to the measurement at 105 amu (de Gouw et al., 2003a). In most air masses, a PTR-MS measurement at 105 amu cannot be expected to be unique for either species. Close to emission sources (petrochemical industry, tunnel studies) styrene probably dominates the measurement. In well-aged air masses, PiBN is probably much higher than styrene, but the levels will also be close to the detection limits of the PTR-MS.

16. Mass 107: C_8-aromatics

GC-PTR-MS analyses of urban air have shown that four different species contribute to the measurement at 107 amu: ethyl benzene, (m + p)-xylene and o-xylene. In addition, an occasional small peak from benzaldehyde is observed by GC-PTR-MS. A number of inter-comparisons between the PTR-MS measurement at 107 amu and the sum measurements of these four species have been performed with widely different results (Table 2). An earlier inter-comparison from our laboratory indicated a good correlation but a poor quantitative agreement, which we attributed to calibration inaccuracies (de Gouw et al., 2003a). Indeed, later work with newly obtained standards gave a much better agreement with an alternative method (Fig. 11) (de Gouw et al., 2006). Other published results have revealed some discrepancies (Steinbacher et al., 2004), and it would be good to understand these in more detail.

17. Mass 121: C_9-aromatics

GC-PTR-MS analyses of urban air show that a number of different species contribute to the measurement at 121 amu: two propyl benzene, two ethyl toluene, and three trimethyl benzene isomers. Inter-comparisons between the PTR-MS measurement and GC measurement of all these species individually have shown good correlations, but the quantitative agreement was only good to within a factor of 2 (Table 2). The agreement is limited by the fact that 7 different C_9-aromatics have to be determined accurately for the inter-comparison. Several studies have indicated that there is a non-zero offset at 121 amu, which we attributed to the presence of $C^{35}Cl^{37}Cl_2^+$ ions from CCl_4 (Spanel & Smith, 1999). The interference from CCl_4 is expected to be a constant offset in the measurement, since the atmospheric variability of CCl_4 is very low.

18. Mass 137: Monoterpenes

Several monoterpenes are detected at 137 amu in PTR-MS. Four inter-comparisons have been reported (Table 2), and in three of four studies the agreement was within 30%. In this case, the monoterpene measurement by PTR-MS is compared with the measurement of the sum of up to six different monoterpenes, and due to the propagation of errors an agreement better than 30% cannot be expected. An important fragment from monoterpenes is detected at 81 amu, which mass also seems to be unique to monoterpenes (de Gouw et al., 2003a; Rinne et al., 2005). The effects of humidity on the detection of monoterpenes were investigated in detail and found to be relatively minor (Tani et al., 2004).

19. Other Masses

Numerous other masses have been used in PTR-MS measurements of atmospheric VOCs, and the identifications are summarized in Table 3. In many of these cases the identification

TABLE 3. Published identifications of masses detected by PTR-MS in ambient air

Mass (amu)	Compound	Reference
28	HCN	(Karl et al., 2003)
30	HONO	(Wisthaler et al., 2003)
31	Formaldehyde	chapter III
33	Methanol	id.
42	Acetonitrile	id.
43	Multiple species	id.
45	Acetaldehyde	id.
47	Formic acid	(Williams et al., 2001; Karl et al., 2004)
54	Acrylonitrile	(Karl et al., 2003)
57	Butenes, MTBE, butanol	(Karl et al., 2003)
59	Acetone	chapter III
61	Acetic acid	id.
63	DMS	id.
69	Isoprene	id.
	Furan	id.
71	MVK + MACR	id.
73	MEK	id.
75	Hydroxy acetone	(Williams et al., 2000; Williams et al., 2001)
77	PAN	chapter III
79	Benzene	id.
81	Monoterpenes	id.
	Hexenal	(Karl et al., 2001c; Karl et al., 2001d; Warneke et al., 2002)
83	Hexenol, hexanal, hexenyl acetate	(Karl et al., 2001a; Karl et al., 2001c; Karl et al., 2001d; Karl et al., 2001e; Williams et al., 2001)
	Methyl furan, isoprene hydroxy carbonyls	(Williams et al., 2001)
85	Ethyl vinyl ketone	(Karl et al., 2001a)
87	MBO	(Holzinger et al., 2005a)
	C_5-carbonyls, methacrylic acid	(Williams et al., 2001)
91	PPN	(Hansel & Wisthaler, 2000)
93	Toluene	chapter III
95	2-vinyl furan	(Williams et al., 2001)
	Phenol	(Rinne et al., 2005)
99	Hexenal	(Karl et al., 2001a; Karl et al., 2001d; Williams et al., 2001; Warneke et al., 2002)
101	Isoprene hydroperoxides	(Crutzen et al., 2000; Williams et al., 2000; Warneke et al., 2001a; Williams et al., 2001)
103	MPAN	(Hansel & Wisthaler, 2000)
105	Styrene, PiBN	chapter III
107	C_8-aromatics	id.
115	Heptanal	(Karl et al., 2001a)
121	C_9-aromatics	chapter III
129	Octanal	(Karl et al., 2001a)
	Naphthalene	(Karl et al., 2003)
135	C_{10}-aromatics	(Karl et al., 2001b; Beauchamp et al., 2004)
137	Monoterpenes	chapter III
139	Nopinone	(Holzinger et al., 2005a)
143	Nonanal	(Karl et al., 2001a)
149	C_{11}-aromatics	(Karl et al., 2003)
	Methylchavicol	(Holzinger et al., 2005a)
151	Pinonaldehyde	(Holzinger et al., 2005a)
163	C_{12}-aromatics	(Karl et al., 2003)

of the masses is more tentative: they are based on the variability of the signal in time, space and with altitude, and on the covariance with other measurements. Many of these identifications could be very specific for certain air masses, and have a very limited applicability to other regions of the atmosphere. The reader is referred to the papers cited in Table 3 for more details. Table 3 points out that there is still a wealth of information contained in masses other than those discussed above, which should be explored in more detail in future studies. Numerous papers have examined the release of VOCs from various atmospheric sources using laboratory measurements with PTR-MS. A highly relevant study in this regard is the work by Yokelson and co-workers, who studied the specificity of PTR-MS in laboratory studies of fire emissions (Christian et al., 2004).

IV. RESEARCH HIGHLIGHTS

A. Atmospheric Measurements Onboard Aircraft, Ships and Vehicles

Some of the major contributions of PTR-MS to atmospheric research have come through its use onboard research aircraft. PTR-MS allows the airborne monitoring of VOCs with a fast time response, which results in a good data coverage across horizontal distances and different altitudes. To give some examples: during the ICARTT mission in 2004, our PTR-MS monitored a total of 16 masses at 1 sec each, adding up to cycle time of ~18 sec. In 18 sec the aircraft moved ~2.2 km horizontally and ~90 m vertically when climbing or descending. The use of PTR-MS onboard an aircraft is not very labor intensive and can be automated. As a result, a modestly sized research group can accomplish more than 1 mission a year, including the time needed for reduction of the data.

Several groups have used PTR-MS for airborne measurements of VOCs and Table 4 lists the projects, locations, and resulting publications. Other groups that have deployed PTR-MS on aircraft include Karl et al. onboard a Brazilian aircraft over the rainforest in South America, Jobson et al. onboard the DOE G-1 over the Vancouver area and the northeastern US, and Oram et al. onboard the British BAE-146 aircraft over the mid-Atlantic. At this point, publications describing these measurements have not appeared in the peer-reviewed literature. In addition to the aircraft measurements, PTR-MS instruments have been successfully deployed onboard several research ships (see Table 5 for a list of projects, locations, and resulting publications), and inside the Aerodyne mobile laboratory (Herndon et al., 2005; Jiang et al., 2005).

In this section we will review some of our findings from the airborne research for biomass burning and urban plumes. The data were obtained onboard the NOAA WP-3D research aircraft during the ITCT 2k2 (Intercontinental Transport and Chemical Transformation) study in 2002, and the ICARTT study in 2004. The major goal of the ITCT 2k2 mission was to study the transport of polluted air from Asia across the Pacific Ocean to the western United States (de Gouw et al., 2004a). The ICARTT collaboration involved an air quality study in the northeastern United States as well as long-range transport study of North American pollution across the Atlantic Ocean.

B. Biomass Burning Plumes

Early measurements of acetonitrile (CH_3CN) in the atmosphere indicated that biomass burning was one of the main sources of this inert VOC (Arijs & Brasseur, 1986; Hamm & Warneck, 1990). PTR-MS allows measurements of acetonitrile, and these have proven to be highly valuable in identifying biomass-burning plumes in the atmosphere. Laboratory analyses by PTR-MS confirmed that acetonitrile was strongly emitted by the burning of biofuels (Holzinger et al., 1999; Christian et al., 2003, 2004), whereas field studies demonstrated that other sources of this compound were minor (Holzinger et al., 2001; de Gouw et al., 2003c, 2006). As a result, acetonitrile measurements by PTR-MS have proven to be useful to identify biomass-burning plumes during multiple airborne studies (Andreae et al., 2001; Holzinger et al., 2005b; de Gouw et al., 2006). In addition, acetonitrile measurements were used to estimate the contribution of biomass burning to the atmosphere over the Indian Ocean (Lelieveld et al., 2001), the eastern Pacific (de Gouw et al., 2004a) and the northeastern US (Warneke et al., 2006). The results of several PTR-MS measurements have indicated that acetonitrile is lost at the surface of the ocean (de Laat et al., 2001; Warneke & de Gouw, 2001; de Gouw et al., 2003c), but there are also some suggestions of an ocean source (Sanhueza et al., 2004).

During the ITCT 2k2 study the NOAA WP-3D aircraft sampled a forest fire plume over Utah (Fig. 17). The fire was observed from the aircraft, and the smoke was sampled at 5 km altitude in a relatively clean region of the troposphere. The flight track is shown in Figure 17 and is color-coded by the measured mixing ratio of acetonitrile. The location of the fire plume is clearly seen from the strong acetonitrile enhancement. Back-trajectories from the sampling location suggested that the smoke had been transported for approximately 2 hr before being sampled by the aircraft (Fig. 17).

During the ICARTT study, large-scale forest fires were burning in Alaska and western Canada, and the emissions were sampled on multiple flights of the NOAA WP-3D (de Gouw et al., 2006). The highest concentrations of acetonitrile were measured over eastern Canada on July 9, 2004, and the flight track is shown in Figure 17. A back-trajectory calculated from the location of the highest acetonitrile (Fig. 17) leads back to the region where forest fires were detected with the MODIS satellite instrument, indicated by the blue triangles in Figure 17. A more detailed meteorological analysis using the Lagrangian transport model FLEXPART confirms that the NOAA WP-3D sampled the emissions from these fires on July 9, 2004, after a transport time of 6–10 days (de Gouw et al., 2006).

Figure 18 shows the results of the PTR-MS measurements in the two fire plumes discussed in the previous paragraph. Panel A shows that acetonitrile was strongly enhanced in both plumes with peak values well over 1 ppbv, and also well correlated with CO. The enhancement ratio of acetonitrile versus CO is determined by the slope of a scatter plot of the two species and is given in Table 6. These enhancement ratio values were also presented elsewhere (de Gouw et al., 2003c, 2006). Panel B shows the measurements of aromatic species in the plumes, and it is seen that benzene is the most abundant. Toluene is lower than benzene in the Utah plume, and is even more reduced in the Alaska plume. The latter difference can be explained by chemical

TABLE 4. Airborne measurements using PTR-MS

Project	Location	Aircraft	References
Lindinger and Hansel			
LBA-Claire	Surinam	Citation II	(Crutzen et al., 2000; Williams et al., 2000; Andreae et al., 2001; Poschl et al., 2001; Warneke et al., 2001a; Williams et al., 2001)
INDOEX	Indian Ocean	NCAR C-130	(Sprung et al., 2001)
TexAQS	Texas	NCAR Electra	(Hawes et al., 2003; Wert et al., 2003)
De Gouw and Warneke			
INDOEX	Indian Ocean	Citation II	(de Gouw et al., 2001; Lelieveld et al., 2001)
MINOS	Mediterranean Sea	DLR Falcon	(Lelieveld et al., 2002; de Reus et al., 2003; Fischer et al., 2003; Kormann et al., 2003; Scheeren et al., 2003; Traub et al., 2003; de Gouw et al., 2004b)
ITCT 2k2	Eastern Pacific	NOAA WP-3D	(de Gouw et al., 2003c; Brock et al., 2004; Cooper et al., 2004; de Gouw et al., 2004a; Hudson et al., 2004; Northway et al., 2004; Nowak et al., 2004; Roberts et al., 2004; Jacob et al., 2005)
ICARTT	Northeastern U.S.	NOAA WP-3D	(Brown et al., 2005; de Gouw et al., 2006; Warneke et al., 2006)
Williams et al.			
MINOS	Mediterranean Sea	DLR Falcon	(Lelieveld et al., 2002; de Reus et al., 2003; Fischer et al., 2003; Kormann et al., 2003; Scheeren et al., 2003; de Gouw et al., 2004b; Holzinger et al., 2005b)

TABLE 5. Ship-based measurements using PTR-MS

Project	Location	Ship	References
Lindinger and Hansel			
INDOEX	Indian Ocean	NOAA Ronald H. Brown	(Lelieveld et al., 2001; Wisthaler et al., 2002; Guazzotti et al., 2003)
De Gouw and Warneke			
	Indian Ocean	NIOZ Pelagia	(Warneke & de Gouw, 2001)
NEAQS 2002	Gulf of Maine	NOAA Ronald H. Brown	(de Gouw et al., 2003a; Warneke et al., 2004a; de Gouw et al., 2005)
Williams et al.			
	Atlantic Ocean	Meteor	(Williams et al., 2004)

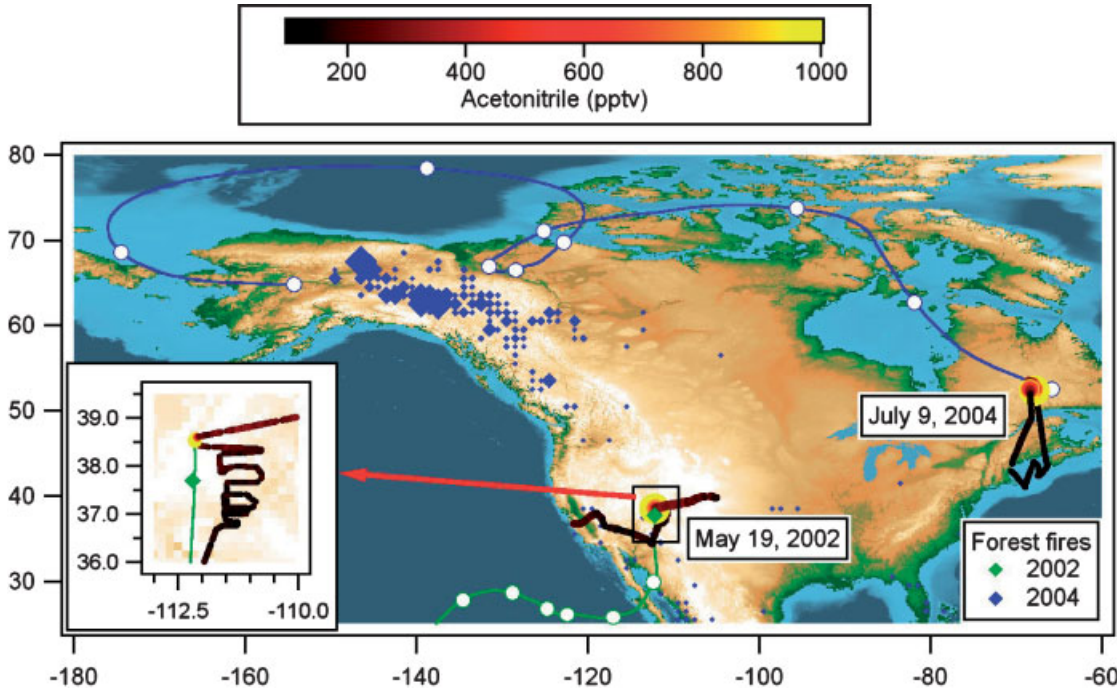

FIGURE 17. Sampling locations of two fire plumes observed from the NOAA WP-3D. The flight tracks are color-coded by the measured acetonitrile mixing ratio. The first plume was observed over Utah in 2002. The location of the fire is indicated by the green triangle. The second plume was observed over eastern Canada, and had come from Alaska where the fire locations are indicated by the blue triangles. The green and blue curves show back-trajectories from the sampling location with the highest acetonitrile with one symbol every 24 hr.

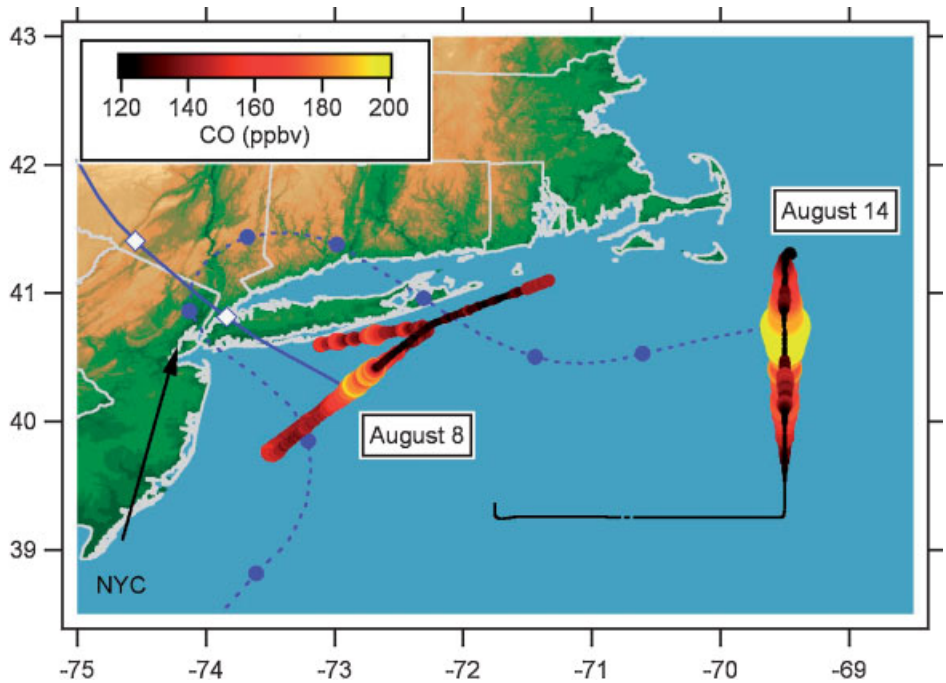

FIGURE 19. Sampling locations of two urban plumes from New York City. The plumes observed on August 8 and 14, 2004, were observed at night and day, respectively. The map shows part of the flight tracks of the NOAA WP-3D color-coded by the CO measurement. The blue curves show back-trajectories with 1 symbol per 4 hr. (CO data are courtesy of John Holloway).

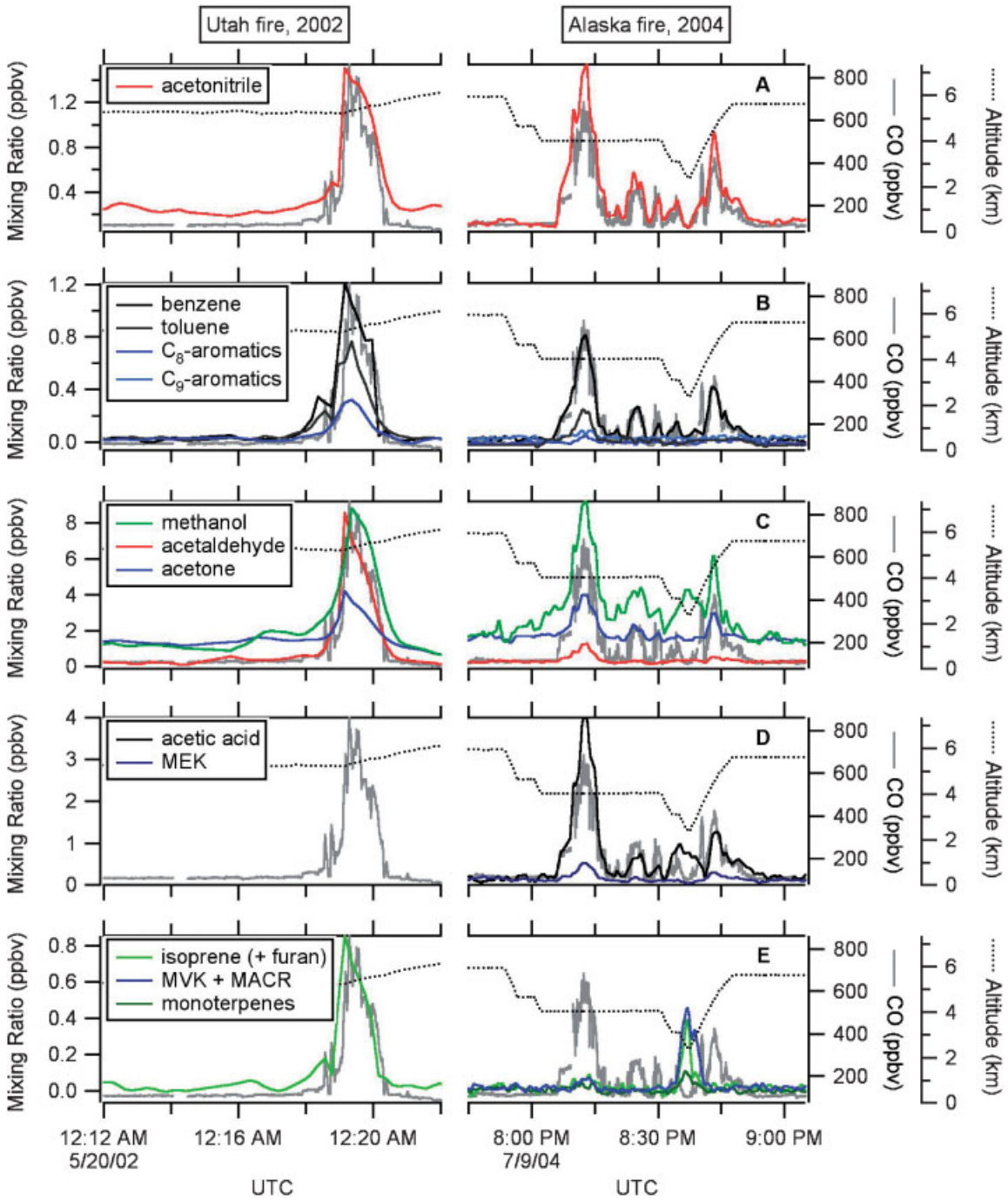

FIGURE 18. PTR-MS measurement results from a relatively unprocessed fire plume over Utah in 2002 (**left panels**), and an aged fire plume from Alaska observed over eastern Canada in 2004 (**right panels**). (CO data are courtesy of John Holloway).

removal, since toluene is more reactive than benzene and CO (Atkinson & Arey, 2003). Even more reactive are the C_8-aromatics; as a result they have been largely removed from the Alaskan plume. Panel C shows the measurements of methanol, acetaldehyde, and acetone. Methanol and acetone are relatively inert and show very similar enhancement ratios in the Utah and Alaska plumes, in contrast with observations in the Mediterranean (Holzinger et al., 2005b). Acetaldehyde is much more reactive and is reduced in the Alaska plume as a result. Panel D shows the measurement results for acetic acid and MEK, which were only measured in the Alaska plume. Acetic acid in particular is strongly enhanced, and both species are well correlated with CO. Panel E shows the measurement results of isoprene, MVK + MACR, and the monoterpenes. The signal for

TABLE 6. VOC enhancement ratios versus CO, in pptv/ppbv, determined in 2 forest fire, and 2 urban plumes

VOC	Forest fire plumes		Urban plumes	
	Utah	Canada	New York City	New York City
	May 19, 2002	July 9, 2004	August 8, 2004	August 14, 2004
Methanol	12.4	12.4	11.3	4.4
Acetonitrile	2.0	2.55	0.2	0
Acetaldehyde	11.2	1.68	3.5	4.1
Acetone	4.4	4.82	4.3	12.0
Acetic acid	n/a	6.4	1.8	4.3
Isoprene	1.1 [a]	0.12	0.4	0.13
MVK + MACR	n/a	0.11	2.8	0.53
MEK	n/a	0.78	1.0	2.4
Benzene	1.7	1.41	0.98	0.96
Toluene	1.0	0.44	2.4	0.76
C_8-aromatics	0.45	0.071	1.9	0.19
C_9-aromatics	n/a	0.097	1.7	0.12
Monoterpenes	n/a	0.06	0.2	0

[a]The signal at 69 amu may consist of furan and isoprene. See text for more details.

isoprene was enhanced in the Utah plume, but in this case there is most likely a large contribution from furan to the signal (Christian et al., 2004). Indeed, adding up the emission ratios for isoprene (0.17–0.38 pptv/ppbv) and furan (0.60–1.50 pptv/ppbv) reported for fires in Montana, Colorado and California (Friedli et al., 2001) gives a range of values that includes the ratio of 1.1 pptv/ppbv determined here (Table 6). The biogenic VOCs showed very small enhancements in the Alaska plume: these species are very reactive and typically do not survive a multi-day transport. The biogenic VOCs did show an enhancement, however, in the continental boundary layer (CBL) underneath the fire plume where CO and acetonitrile were at a minimum. Interestingly, methanol and acetic acid, which have been suggested to have primary and/or secondary biogenic sources (de Gouw et al., 2005), also show enhancements in the CBL (Fig. 18C,D).

A more detailed analysis of the chemical differences between the Utah and Alaska plume is beyond the scope of this paper, and has been presented elsewhere (de Gouw et al., 2006). The enhancement ratios observed in the Utah plume were largely consistent with published emission ratios. The chemical removal for each VOC was described versus transport time, and was consistent with the known OH removal rates. From the presence of reactive VOCs, such as acetaldehyde and toluene, in the Alaska plume it was inferred that the average concentration of OH had been low during the transport.

C. Urban Plumes

During the ITCT 2k2 and ICARTT studies, the NOAA WP-3D sampled numerous urban plumes, and two examples are given in Figure 19. A nighttime flight was conducted on August 7–8, 2004, which allowed urban air to be sampled with a minimum of processing during the transport. Figure 19 shows part of the flight track color-coded by CO. Enhanced CO was observed southeast of New York City, and a back-trajectory leads back to the city and shows that the transport time was ~4 hr. The plume was observed at 2:15 am UTC or 10:15 pm local time, and thus the observed pollutants were emitted around 6:15 pm, and transported at a time when the atmospheric oxidation by OH and NO_3 is at a minimum (Warneke et al., 2004a). On August 14, 2004, a plume from New

York City was intercepted to the east during a daytime flight. The back-trajectory in Figure 19 shows that the plume had been transported for ~24 hr.

Figure 20 shows the results from the PTR-MS measurements in the two urban plumes discussed in the previous paragraph. Enhancement ratios for all VOCs versus CO are given in Table 6. The urban plumes are readily discerned from the forest fire plumes in Figure 18 by the absence of acetonitrile (Fig. 20C). In addition, the ratios between the aromatic VOCs are quite different: benzene is the dominant aromatic VOC in the unprocessed forest fire plume (Fig. 18B), whereas toluene is dominant in the unprocessed urban plume (Fig. 20A).

The night- and day-time plumes from New York City show some striking chemical differences. The highest enhancement ratios of aromatic VOCs (Table 6) are observed in the nighttime plume. For toluene and in particular the higher aromatics, much lower values are seen in the daytime plume, explained by reactions with OH during the transport. In contrast, the enhancement ratios of the oxygenated VOCs are much lower in the nighttime plume than in the daytime plume. This is particularly the case for acetone, acetic acid, and MEK, and to a lesser extent for acetaldehyde (Fig. 20B,C). These observations are largely consistent with the evolution of aromatic and oxygenated VOCs in urban plumes inferred from ship-based measurements in 2002 (de Gouw et al., 2005): aromatics are removed from the atmosphere in reactions with OH, whereas oxygenated VOCs are also photo-chemically produced.

The levels of biogenic VOCs were low but not zero in the urban plumes (Fig. 20D). This could be due to emissions from urban vegetation. Biogenic emissions are not limited to city boundaries, and as a result, the correlation with CO is not as good as for the anthropogenic VOCs. During the nighttime flight, the levels of MVK + MACR were much higher than those of their precursor, isoprene. This indicates a high degree of photochemical processing of the biogenic emissions, as expected for emissions that take place mainly during the day and are measured during the night. The levels of biogenic VOCs were even lower in the daytime plume, which was exposed to much higher concentrations of OH radicals during the transport.

A more detailed analysis of the chemical differences between the night- and daytime plumes observed during ICARTT is beyond the scope of this paper and will be presented elsewhere. It should be noted that the observations reported in Figure 20 and Table 6 were very typical for the VOC composition of urban plumes during ICARTT, and largely consistent with previous work (de Gouw et al., 2005).

V. RECENT INSTRUMENT DEVELOPMENTS

A. Improvement of the Sensitivity

Equation (2.15) shows that to improve the sensitivity of a PTR-MS instrument, one can try to improve the total H_3O^+ signal. Ionicon made significant progress in this regard by adding a third turbo pump to the system, which added a differentially pumped stage between the drift tube and the quadrupole mass spectrometer chamber. This allowed the ion sampling orifices to be made larger and the ion sampling efficiencies to be higher by a factor of 3–4. In addition, the sensitivity can be improved by increasing the pressure and/or the length of the drift tube. If the same *E/N* ratio is maintained, the sensitivity is linear in the length and the pressure of the drift tube.

We explored increasing the length of the drift tube and built a reactor of 50 cm (de Gouw et al., 1999, 2000). The overall drift-tube voltage needs to be increased proportionally with the length. In a standard PTR-MS with a 10 cm reactor, the drift-tube voltage is between 600 and 800 V, so for a 50 cm reactor it needs to be 3–4 kV. With these high voltages, the discharge of voltages across parts of the drift tube are much more difficult to avoid, and we found little advantage with using longer drift tubes.

A PTR-MS instrument with an increased drift tube pressure of 13 mbar and a radioactive ion source was developed at NCAR (Hanson et al., 2003). These authors reported sensitivities for acetone of 240 cps/ppbv at a H_3O^+ ion signal of 10^6 cps, which is a factor of 4–5 higher than in a standard PTR-MS. This instrument was recently used to measure the VOCs from vegetation heated in an oven to mimic the effects of a wildfire (Greenberg et al., 2005). The H_3O^+ signal reported was relatively low at 2×10^6 cps, and the advantage over a standard PTR-MS instrument was relatively small. This approach holds a similar disadvantage as increasing the length: the electric field must be increased proportionally with the pressure to operate at the same *E/N* value, and discharges start to become a problem. Nevertheless, the use of higher pressures is a promising improvement that could be further explored.

Finally, the use of lower *E/N* values could be explored in more detail. To avoid problems with cluster-ion formation (see, e.g., Fig. 12), one could develop a drift-tube design with a low-*E/N* region for an efficient ionization of VOCs, and a high-*E/N* region to dissociate the cluster ions from the low-*E/N* region. A disadvantage of such an approach is that it changes the ion chemistry considerably: a much higher fraction of $H_3O^+(H_2O)_n$ ions will be present in the low-*E/N* region. Most oxygenated VOCs react efficiently with both H_3O^+ and $H_3O^+(H_2O)_n$ ions, and for those species an improvement in the sensitivity is expected. For aromatic species, however, the reactions with $H_3O^+(H_2O)_n$ ions are less efficient and the sensitivity would actually be reduced.

B. Ion-Trap Mass Spectrometry

In PTR-MS only the mass of product ions is determined, which is a useful but not a unique indicator of the identity of a VOC. The presence of different species of the same mass, product ion fragmentation, and cluster ion formation can all lead to significant mass overlap. This complicates the interpretation of the product ion signals, particularly in cases where no prior knowledge of the VOC composition exists. To overcome these disadvantages, we have developed a proton-transfer ion-trap mass spectrometry instrument (PIT-MS), which uses an ion trap mass spectrometer instead of the quadrupole mass filter in a standard PTR-MS (Warneke et al., 2004b, 2005a). A similar instrument was developed by Alexander and co-workers (Prazeller et al., 2003), albeit with a lower sensitivity. In the PIT-MS, ions of one particular mass can be collected in the ion trap, and can then be fragmented in collisions with the buffer gas.

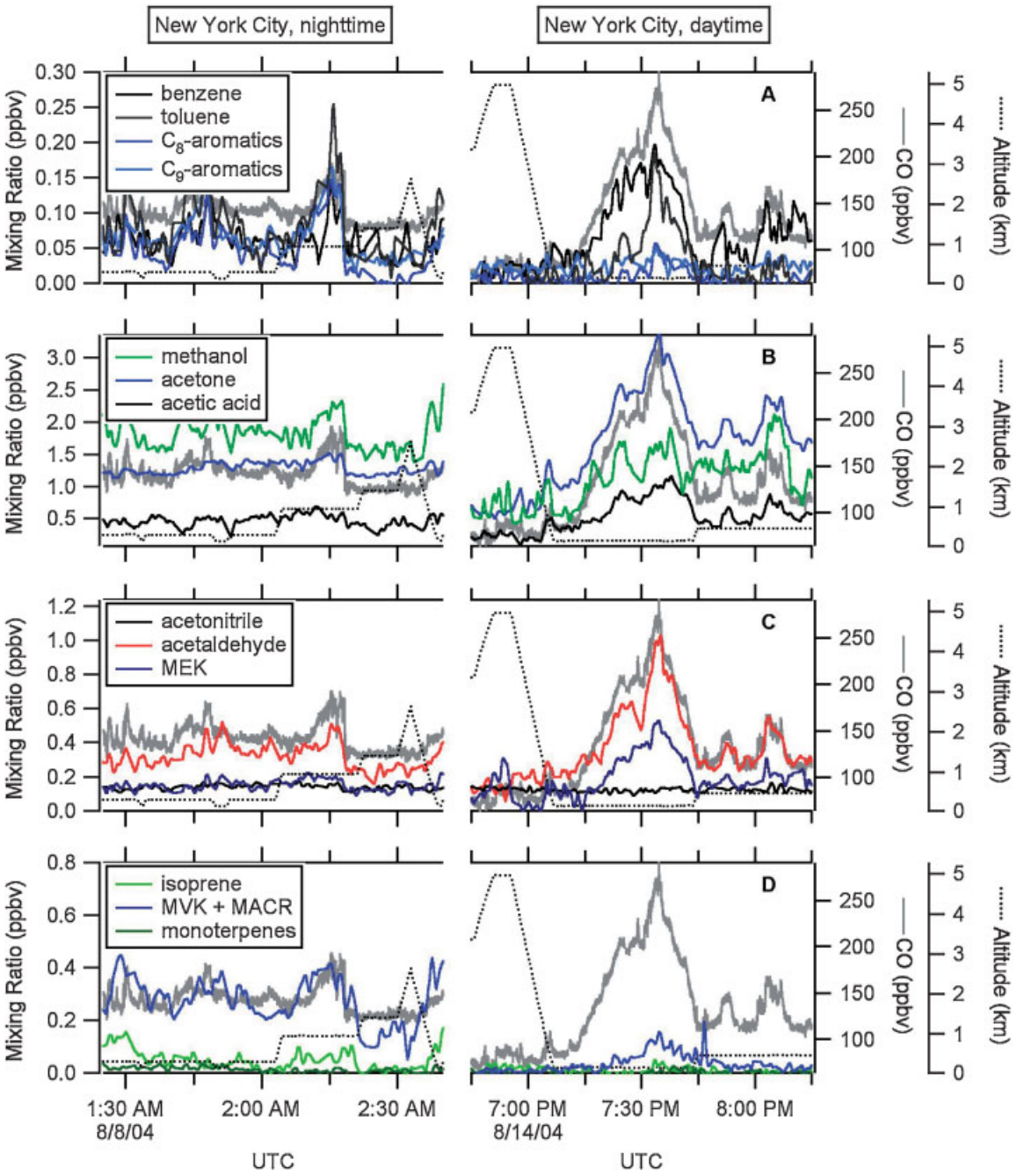

FIGURE 20. PTR-MS measurement results from a relatively unprocessed, nighttime plume (**left panels**) and a well-processed, daytime plume (**right panels**) from New York City. (CO data are courtesy of John Holloway).

Different product ions of the same mass can yield different ion fragments, thus providing a means to distinguish between them. Triple quadrupole mass spectrometers and linear ion traps can be used to construct instruments similar to the PIT-MS, but have not been described in the literature.

A detailed description of the PIT-MS instrument developed in our laboratory is beyond the scope of this review and has been given elsewhere (Warneke et al., 2005a). Briefly, the discharge ion source and drift tube reactor are similar to those in a PTR-MS. The ions that are extracted from the drift tube are focused onto the entrance of the ion trap by a set of electrostatic lenses. The trap consists of a ring and two end-cap electrodes. A radio-frequency (RF) voltage is supplied to the ring electrode and provides the trapping field. A kHz-frequency voltage generated with a computer-controlled function generator can be supplied to the two end-cap electrodes. This allows selecting a specific range of

masses to be trapped, and is also used to fragment the ions at one mass.

An example of how the system works is shown in Figure 21. Figure 21A shows the mass spectrum generated when zero air with a trace amount of acetone is added to the PIT-MS. The mass spectrum contains several peaks including the $H_3O^+(H_2O)_n$ ion clusters ($n = 1–3$) and the $H^+(CH_3COCH_3)_n$ ions ($n = 1–2$); the H_3O^+ peak at 19 amu was not measured in this scan. Using a filtered-noise field on the end caps, the trap can be made unstable for all ions except the $H^+(CH_3COCH_3)$ ions at 59 amu, and the resulting mass spectrum is shown in Figure 21B. In the final step a kHz voltage that is resonant with the motion of the ions at 59 amu is applied to the end caps. As a result, the kinetic energy of those ions is increased and they fragment in collisions with the He buffer gas. The resulting spectrum of fragment ions is shown in Figure 21C. The $H^+(CH_3COCH_3)$ ions give five different fragments, of which the ions at 31 and 41 amu are the main channels.

The PIT-MS was inter-compared with a PTR-MS instrument during a ground-based measurement in our Boulder laboratory (Warneke et al., 2005a), and with a GC-MS instrument onboard the NOAA research ship Ronald H. Brown (Warneke et al., 2005b). In both cases the PIT-MS instrument compared well with the other instrument. Collision-induced dissociation measurements turned out to be useful to distinguish between acetone and propanal (Warneke et al., 2005a,b) and between two different hexenal isomers (Karl et al., 2005).

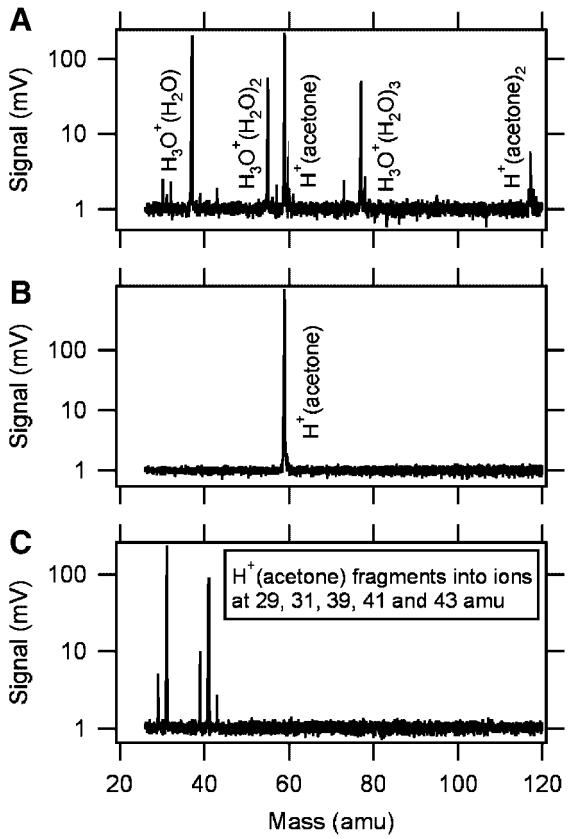

FIGURE 21. Principle of a collision-induced dissociation measurement.

Proton-transfer reactions inside the ion trap can potentially be used to differentiate between ions of the same mass. Warneke et al. have shown that by adding a reagent VOC to the He buffer gas, VOCs with a lower proton affinity than that of the reagent will remain in the trap, whereas VOCs with a higher proton affinity will react with the reagent and form ions at a different mass (Warneke et al., 2004b). In specific cases, this method may be more selective than the use of collision-induced dissociation. Much more work is needed to explore this option in detail.

C. Time-of-Flight Mass Spectrometry

Time-of-flight mass spectrometry (TOF-MS) eliminates the need to select a subset of ions to be monitored prior to an experiment. In addition, TOF-MS has a superior mass resolution, which allows the mass separation of nominally isobaric ions. Both advantages would be of great interest in PTR-MS, provided they could be incorporated without a significant loss of sensitivity. Blake et al. were the first to report the use of a TOF-MS in a PTR-MS instrument (Blake et al., 2004). However, the sensitivity reported was low at 0.17 cps/ppbv for H_2S, and must be significantly improved to detect VOCs in ambient air with a high time resolution. Ennis et al. reported on the development of a PTR-TOF instrument with a reflectron TOF mass spectrometer (Ennis et al., 2005). The high mass resolution allowed the separation of nominally isobaric ions, protonated ethanol and formic acid, but the sensitivity was low in comparison with PTR-MS instruments. Inomata et al. reported the development of a PTR-TOF-MS instrument with a novel discharge ion source, a higher drift tube pressure and a detection limit below 1 ppbv for 1-min integration times (Inomata et al., 2006). A disadvantage of TOF-MS is that the ions need to be pulsed into the time-of-flight region. In a PTR-MS instrument a constant current of primary and product ions is generated, and injecting them into a TOF-MS as ion pulses can only be done at the cost of some ion losses. It may be possible to overcome these disadvantages by using the higher duty-cycle TOF-MS system designed by Tofwerk, which has been successfully incorporated into aerosol mass spectrometry (AMS) instruments (Drewnick et al., 2005), or by using the so-called Hadamard transform TOF-MS method developed by Zare and co-workers (Zare, Fernandez, & Kimmel, 2003).

D. Other Reagent Ions

Surprisingly little work has been done to use ions different from H_3O^+ as reagent in a PTR-MS. The advantages could be two-fold. First, by using a reagent ion consisting of a proton bound to a neutral with a higher proton affinity, the proton transfer becomes more selective, and the product ion signals would be easier to interpret. An example is the use of protonated hydrazine, $N_2H_5^+$, which reacts differently with nominally isobaric aldehydes and ketones (Morrison & Howard, 2001). Second, the bond energy between H_3O^+ and H_2O is relatively high and, therefore, a high *E/N* needs to be used to prevent the reagent ions from clustering. By using a different reagent ion, the instrument could probably run at a lower *E/N*, which would result in an improved sensitivity. In practice, it may not be easy to generate different reagent ions

cleanly in the hollow-cathode discharge ion source used in PTR-MS, but more work can and should be done.

VI. CONCLUSION AND FUTURE OUTLOOK

This review has demonstrated that atmospheric applications of PTR-MS have reached a mature state: the instrument's response for different species has been characterized in detail, and the measurements that have been reported are generally accurate within 20%. Nevertheless, much more work can and should be done. For example, the response for two important atmospheric species, formaldehyde and PAN, should be investigated in more detail, and the measurements should be inter-compared versus alternative methods. Also, the measurements of acetic and possibly formic acid should be better calibrated and inter-compared versus alternative techniques. GC-PTR-MS analyses have been mostly restricted to winter-time urban atmospheres, and should be performed for air samples from other regions of the atmospheres, including those that are impacted by biomass burning emissions, and the vegetation in different ecosystems. Research will continue to improve PTR-MS instruments, including the use of time-of-flight, and (linear) ion trap mass spectrometers. New directions that are currently being explored include the on-line analysis of atmospheric aerosol.

Atmospheric measurements using PTR-MS onboard aircraft, ships and at ground sites have given a wealth of information about the emissions and atmospheric formation of VOCs. However, our current understanding is still limited for the oxygenated species. The atmospheric mixing ratios of acetaldehyde, for example, are difficult to explain using the best available estimates of its sources and chemistry. More research is needed in the laboratory to characterize the response of PTR-MS for this important VOC, in particular in conditions with high levels of oxidants such as ozone. Measurements of acetaldehyde in the free troposphere should be inter-compared carefully versus other techniques.

PTR-MS has become a useful tool for atmospheric research because it gives a chemical fingerprint of the origin and history of an air mass. Air masses impacted by forest-fire, urban, marine, and vegetation emissions can be readily distinguished from another, and the degree of photochemical processing can be inferred from the data. This kind of information has proven to be useful in many studies other than those aimed specifically at VOCs.

ACKNOWLEDGMENTS

We are indebted to the late Werner Lindinger, and to Armin Hansel and Alfons Jordan for developing PTR-MS into the useful and robust research tool that it has become. Several colleagues recognized the possibilities of PTR-MS for atmospheric research at an early stage and were instrumental in the development of this work. Those people included Paul Crutzen and Jos Lelieveld of the Max Planck Institute for Chemistry in Mainz, Henrik Rudolph, and Arend Niehaus of the University of Utrecht, Ray Fall of the University of Colorado in Boulder, Carl Howard and Fred Fehsenfeld of the NOAA Aeronomy Laboratory, and Alex Guenther of NCAR. We are fortunate to have collaborated with Carina van der Veen, Bert Scheeren, and Michel Bolder at the University of Utrecht, and with Bill Kuster, Paul Goldan, and Ned Lovejoy at the NOAA Aeronomy Laboratory, who all greatly contributed to this work. We gratefully acknowledge the helpful PTR-MS discussions over the years with many colleagues, including Michael Alexander, Josef Dommen, David Fahey, Allen Goldstein, David Hanson, Frans Harren, Rupert Holzinger, Greg Huey, Thomas Karl, Shuji Kato, Berk Knighton, Makoto Koike, Megan Northway, Peter Prazeller, Troy Thornberry, Jonathan Williams, and Armin Wisthaler. Additional data were kindly provided by Elliot Atlas of the University of Miami, Hans Schlager of the DLR, and John Holloway and Paul Goldan of NOAA. Finally, we thank both reviewers for useful feedback on this paper.

REFERENCES

Ammann C, Spirig C, Neftel A, Steinbacher M, Komenda M, Schaub A. 2004. Application of PTR-MS for measurements of biogenic VOC in a deciduous forest. Int J Mass Spectrom 239:87–101.

Andreae MO, Merlet P. 2001. Emission of trace gases and aerosols from biomass burning. Global Biogeochem Cycles 15:955–966.

Andreae MO, Artaxo P, Fischer H, Freitas SR, Gregoire JM, Hansel A, Hoor P, Kormann R, Krejci R, Lange L, Lelieveld J, Lindinger W, Longo K, Peters W, de Reus M, Scheeren B, Dias M, Strom J, van Velthoven PFJ, Williams J. 2001. Transport of biomass burning smoke to the upper troposphere by deep convection in the equatorial region. Geophysical Res Lett 28:951–954.

Anicich VG. 2003. An index of the literature for bimolecular gas phase cation-molecule reaction kinetics. JPL Publication 03–19:356–390.

Apel EC, Hills AJ, Lueb R, Zindel S, Eisele S, Riemer DD. 2003. A fast-GC/MS system to measure C-2 to C-4 carbonyls and methanol aboard aircraft. J Geophysical Res Atmos 108:8794 doi:10.1029/2002JD003199.

Arijs E, Brasseur G. 1986. Acetonitrile in the stratosphere and implications for positive-ion composition. J Geophysical Res Atmos 91:4003–4016.

Arnold ST, Viggiano AA, Morris RA. 1998. Rate constants and product branching fractions for the reactions of H_3O^+ and NO^+ with C-2-C-12 alkanes. J Phys Chem A 102:8881–8887.

Atkinson R, Arey J. 2003. Atmospheric degradation of volatile organic compounds. Chem Rev 103:4605–4638.

Barker RA, Ridge DP. 1976. Ion-polar neutral momentum transfer collision frequencies: A theoretical approach. J Chem Phys 64:4411–4416.

Beauchamp J, Wisthaler A, Grabmer W, Neuner C, Weber A, Hansel A. 2004. Short-term measurements of CO, $NONO_2$, organic compounds and PM10 at a motorway location in an Austrian valley. Atmos Environ 38:2511–2522.

Blake RS, Whyte C, Hughes CO, Ellis AM, Monks PS. 2004. Demonstration of proton-transfer reaction time-of-flight mass spectrometry for real-time analysis of trace volatile organic compounds. Anal Chem 76:3841–3845.

Brasseur G, Orlando J, Tyndall G. 1999. Atmospheric chemistry and global change. New York: Oxford University Press.

Brock CA, Hudson PK, Lovejoy ER, Sullivan A, Nowak JB, Huey LG, Cooper OR, Cziczo DJ, de Gouw J, Fehsenfeld FC, Holloway JS, Hubler G, Lafleur BG, Murphy DM, Neuman JA, Nicks DK, Orsini DA, Parrish DD, Ryerson TB, Tanner DJ, Warneke C, Weber RJ, Wilson JC. 2004. Particle characteristics following cloud-modified transport from Asia to North America. J Geophysical Res Atmos 109 doi:10.1029/2003JD004198.

Brown SS, Osthoff HD, Stark H, Dube WP, Ryerson TB, Warneke C, de Gouw JA, Wollny AG, Parrish DD, Fehsenfeld FC, Ravishankara AR. 2005. Aircraft observations of daytime NO_3 and N_2O_5 and their implications for tropospheric chemistry. J Photochem Photobiol A-Chem 176:270–278.

Chesnavich WJ, Su T, Bowers MT. 1980. Collisions in a noncentral field: A variational and trajectory investigation of ion-dipole capture. J Chem Phys 72:2641–2655.

Christian TJ, Kleiss B, Yokelson RJ, Holzinger R, Crutzen PJ, Hao WM, Saharjo BH, Ward DE. 2003. Comprehensive laboratory measurements of biomass-burning emissions: 1. Emissions from Indonesian, African, and other fuels. J Geophysical Res Atmos 108 doi:10.1029/2003JD003704.

Christian TJ, Kleiss B, Yokelson RJ, Holzinger R, Crutzen PJ, Hao WM, Shirai T, Blake DR. 2004. Comprehensive laboratory measurements of biomass-burning emissions: 2. First intercomparison of open-path FTIR, PTR-MS, and GC- MS/FID/ECD. J Geophysical Res Atmos 109 doi:10.1029/2003JD003874.

Cooper OR, Forster C, Parrish D, Trainer M, Dunlea E, Ryerson T, Hubler G, Fehsenfeld F, Nicks D, Holloway J, de Gouw J, Warneke C, Roberts JM, Flocke F, Moody J. 2004. A case study of transpacific warm conveyor belt transport: Influence of merging airstreams on trace gas import to North America. J Geophysical Res Atmos 109 doi:10.1029/2003JD003624.

Crutzen PJ, Andreae MO. 1990. Biomass burning in the tropics—Impact on atmospheric chemistry and biogeochemical cycles. Science 250:1669–1678.

Crutzen PJ, Williams J, Poschl U, Hoor P, Fischer H, Warneke C, Holzinger R, Hansel A, Lindinger W, Scheeren B, Lelieveld J. 2000. High spatial and temporal resolution measurements of primary organics and their oxidation products over the tropical forests of Surinam. Atmos Environ 34:1161–1165.

de Gouw JA, Howard CJ, Custer TG, Fall R. 1999. Emissions of volatile organic compounds from cut grass and clover are enhanced during the drying process. Geophysical Res Lett 26:811–814.

de Gouw JA, Howard CJ, Custer TG, Baker BM, Fall R. 2000. Proton-transfer chemical-ionization mass spectrometry allows real-time analysis of volatile organic compounds released from cutting and drying of crops. Environ Sci Technol 34:2640–2648.

de Gouw JA, Warneke C, Scheeren HA, van der Veen C, Bolder M, Scheele MP, Williams J, Wong S, Lange L, Fischer H, Lelieveld J. 2001. Overview of the trace gas measurements on board the citation aircraft during the intensive field phase of INDOEX. J Geophysical Res Atmos 106:28453–28467.

de Gouw JA, Goldan PD, Warneke C, Kuster WC, Roberts JM, Marchewka M, Bertman SB, Pszenny AAP, Keene WC. 2003a. Validation of proton transfer reaction-mass spectrometry (PTR-MS) measurements of gas-phase organic compounds in the atmosphere during the New England Air Quality Study (NEAQS) in 2002. J Geophysical Res Atmos 108:4682 doi:10.1029/2003JD003863.

de Gouw JA, Warneke C, Karl T, Eerdekens G, van der Veen C, Fall R. 2003b. Sensitivity and specificity of atmospheric trace gas detection by proton-transfer-reaction mass spectrometry. Int J Mass Spectrom 223:365–382.

de Gouw JA, Warneke C, Parrish DD, Holloway JS, Trainer M, Fehsenfeld FC. 2003c. Emission sources and ocean uptake of acetonitrile (CH_3CN) in the atmosphere. J Geophysical Res Atmos 108:4329 doi:10.1029/2002JD002897.

de Gouw JA, Cooper OR, Warneke C, Hudson PK, Fehsenfeld FC, Holloway JS, Hubler G, Nicks DK, Nowak JB, Parrish DD, Ryerson TB, Atlas EL, Donnelly SG, Schauffler SM, Stroud V, Johnson K, Carmichael GR, Streets DG. 2004a. Chemical composition of air masses transported from Asia to the US West Coast during ITCT 2K2: Fossil fuel combustion versus biomass-burning signatures. J Geophysical Res Atmos 109 doi:10.1029/2003JD004202.

de Gouw JA, Warneke C, Holzinger R, Klupfel T, Williams J. 2004b. Intercomparison between airborne measurements of methanol, acetonitrile and acetone using two differently configured PTR-MS instruments. Int J Mass Spectrom 239:129–137.

de Gouw JA, Middlebrook AM, Warneke C, Goldan PD, Kuster WC, Roberts JM, Fehsenfeld FC, Worsnop DR, Canagaratna MR, Pszenny AAP, Keene WC, Marchewka M, Bertman SB, Bates TS. 2005. Budget of organic carbon in a polluted atmosphere: Results from the New England Air Quality Study in 2002. J Geophysical Res Atmos 110 doi:10.1029/2004JD005623.

de Gouw JA, Warneke C, Stohl A, Wollny A, Brock C, Cooper O, Holloway J, Trainer M, Fehsenfeld F, Atlas E, Donnelly S, Stroud V, Lueb A. 2006. The VOC composition of merged and aged forest fire plumes from Alaska and western Canada. J Geophysical Res Atmos 111: D10303 doi:10.1029/2005JD006175.

de Laat ATJ, de Gouw JA, Lelieveld J, Hansel A. 2001. Model analysis of trace gas measurements and pollution impact during INDOEX. J Geophysical Res Atmos 106:28469–28480.

de Reus M, Fischer H, Arnold F, de Gouw J, Holzinger R, Warneke C, Williams J. 2003. On the relationship between acetone and carbon monoxide in different air masses. Atmos Chem Phys 3:1709–1723.

Diskin AM, Wang TS, Smith D, Spanel P. 2002. A selected ion flow tube (SIFT), study of the reactions of H_3O^+, NO^+ and O_2^+ ions with a series of alkenes; in support of SIFT-MS. Int J Mass Spectrom 218:87–101.

Dotan I, Albritton DL, Lindinger W, Pahl M. 1976. Mobilities of CO_2^+, N_2H^+, H_3O^+, $H_3O^+H_2O$, and $H_3O^+(H_2O)_2$ Ions in N_2. J Chem Phys 65:5028–5030.

Drewnick F, Hings SS, DeCarlo P, Jayne JT, Gonin M, Fuhrer K, Weimer S, Jimenez JL, Demerjian KL, Borrmann S, Worsnop DR. 2005. A new time-of-flight aerosol mass spectrometer (TOF-AMS)—Instrument description and first field deployment. Aerosol Sci Technol 39:637–658.

Ennis CJ, Reynolds JC, Keely BJ, Carpenter LJ. 2005. A hollow cathode proton transfer reaction time of flight mass spectrometer. Int J Mass Spectrom 247:72–80.

Fischer H, de Reus M, Traub M, Williams J, Lelieveld J, de Gouw J, Warneke C, Schlager H, Minikin A, Scheele R, Siegmund P. 2003. Deep convective injection of boundary layer air into the lowermost stratosphere at midlatitudes. Atmos Chem Phys 3:739–745.

Friedli HR, Atlas E, Stroud VR, Giovanni L, Campos T, Radke LF. 2001. Volatile organic trace gases emitted from North American wildfires. Global Biogeochem Cycles 15:435–452.

Good A, Durden DA, Kebarle P. 1970. Mechanism and rate constants of ion-molecule rfactions leading to formation of $H^+(H_2O)_n$ in moist oxygen and air. J Chem Phys 52:222–229.

Greenberg J, Friedli H, Guenther A, Hanson D, Harley P, Karl T. 2005. Volatile organic emissions from the distillation and pyrolysis of vegetation. Atmos Chem Phys Discuss 5:9097–9126.

Guazzotti SA, Suess DT, Coffee KR, Quinn PK, Bates TS, Wisthaler A, Hansel A, Ball WP, Dickerson RR, Neususs C, Crutzen PJ, Prather KA. 2003. Characterization of carbonaceous aerosols outflow from India and Arabia: Biomass/biofuel burning and fossil fuel combustion. J Geophysical Res Atmos 108 doi:10.1029/2002JD003277.

Guenther A, Hewitt CN, Erickson D, Fall R, Geron C, Graedel T, Harley P, Klinger L, Lerdau M, McKay WA, Pierce T, Scholes B, Steinbrecher R, Tallamraju R, Taylor J, Zimmerman P. 1995. A global-model of natural volatile organic-compound emissions. J Geophys Res Atmos 100: 8873–8892.

Guenther A, Karl T, Harley P, Wiedinmyer C, Palmer PI, Geron C. 2006. Estimates of global terrestrial isoprene emissions using MEGAN (Model of Emissions of Gases and Aerosols from Nature). Atmos Chem Phys Discuss 6:107–173.

Hamm S, Warneck P. 1990. The interhemispheric distribution and the budget of acetonitrile in the troposphere. J Geophysical Res Atmos 95:20593–20606.

Hansel A, Wisthaler A. 2000. A method for real-time detection of PAN, PPN and MPAN in ambient air. Geophysical Res Lett 27:895–898.

Hansel A, Singer W, Wisthaler A, Schwarzmann M, Lindinger W. 1997. Energy dependencies of the proton transfer reactions $H_3O(^+)^+CH_2O$ double left right arrow $CH_2OH^+ + H_2O$. Int J Mass Spectrom 167:697–703.

Hanson D, Greenberg J, Henry B, Kosciuch E. 2003. Proton transfer reaction mass spectrometry at high drift tube pressure. Int J Mass Spectrom 223–224:507–518.

Hawes AK, Solomon S, Portmann RW, Daniel JS, Langford AO, Miller HL, Eubank CS, Goldan P, Wiedinmyer C, Atlas E, Hansel A, Wisthaler A. 2003. Airborne observations of vegetation and implications for biogenic emission characterization. J Environ Monit 5:977–983.

Hayward S, Hewitt CN, Sartin JH, Owen SM. 2002. Performance characteristics and applications of a proton transfer reaction-mass spectrometer for measuring volatile organic compounds in ambient air. Environ Sci Technol 36:1554–1560.

Herndon SC, Jayne JT, Zahniser MS, Worsnop DR, Knighton B, Alwine E, Lamb BK, Zavala M, Nelson DD, McManus JB, Shorter JH, Canagaratna MR, Onasch TB, Kolb CE. 2005. Characterization of urban pollutant emission fluxes and ambient concentration distributions using a mobile laboratory with rapid response instrumentation. Faraday Discuss 130:327–339.

Hewitt CN. 1999. Reactive hydrocarbons in the atmosphere. San Diego: Academic Press.

Hewitt CN, Hayward S, Tani A. 2003. The application of proton transfer reaction-mass spectrometry (PTR-MS) to the monitoring and analysis of volatile organic compounds in the atmosphere. J Environ Monit 5:1–7.

Holzinger R, Warneke C, Hansel A, Jordan A, Lindinger W, Scharffe DH, Schade G, Crutzen PJ. 1999. Biomass burning as a source of formaldehyde, acetaldehyde, methanol, acetone, acetonitrile, and hydrogen cyanide. Geophysical Res Lett 26:1161–1164.

Holzinger R, Jordan A, Hansel A, Lindinger W. 2001. Automobile emissions of acetonitrile: Assessment of its contribution to the global source. J Atmos Chem 38:187–193.

Holzinger R, Lee A, Paw KT, Goldstein AH. 2005a. Observations of oxidation products above a forest imply biogenic emissions of very reactive compounds. Atmos Chem Phys 5:67–75.

Holzinger R, Williams J, Salisbury G, Klupfel T, de Reus M, Traub M, Crutzen PJ, Lelieveld J. 2005b. Oxygenated compounds in aged biomass burning plumes over the Eastern Mediterranean: Evidence for strong secondary production of methanol and acetone. Atmos Chem Phys 5:39–46.

Hudson PK, Murphy DM, Cziczo DJ, Thomson DS, de Gouw JA, Warneke C, Holloway J, Jost JR, Hubler G. 2004. Biomass-burning particle measurements: Characteristic composition and chemical processing. J Geophysical Res Atmos 109 doi:10.1029/2003JD004398.

Hunter EPL, Lias SG. 1998. Evaluated gas phase basicities and proton affinities of molecules: An update. J Phys Chem Ref Data 27:413–656.

Inomata S, Tanimoto H, Aoki N, Hirokawa J, Sadanaga Y. 2006. A novel discharge source of hydronium ions for proton transfer reaction ionization: Design, characterization, and performance. Rapid Commun Mass Spectrom 20:1025–1029.

Jacob DJ, Field BD, Li QB, Blake DR, de Gouw J, Warneke C, Hansel A, Wisthaler A, Singh HB, Guenther A. 2005. Global budget of methanol: Constraints from atmospheric observations. J Geophysical Res Atmos 110 doi:10.1029/2004JD005172.

Jiang M, Marr LC, Dunlea EJ, Herndon SC, Jayne JT, Kolb CE, Knighton WB, Rogers TM, Zavala M, Molina LT, Molina MJ. 2005. Vehicle fleet emissions of black carbon, polycyclic aromatic hydrocarbons, and other pollutants measured by a mobile laboratory in Mexico City. Atmos Chem Phys 5:3377–3387.

Karl T, Crutzen PJ, Mandl M, Staudinger M, Guenther A, Jordan A, Fall R, Lindinger W. 2001a. Variability-lifetime relationship of VOCs observed at the Sonnblick Observatory 1999—Estimation of HO-densities. Atmos Environ 35:5287–5300.

Karl T, Fall R, Crutzen PJ, Jordan A, Lindinger W. 2001b. High concentrations of reactive biogenic VOCs at a high altitude site in late autumn. Geophysical Res Lett 28:507–510.

Karl T, Fall R, Jordan A, Lindinger W. 2001c. On-line analysis of reactive VOCs from urban lawn mowing. Environ Sci Technol 35:2926–2931.

Karl T, Guenther A, Jordan A, Fall R, Lindinger W. 2001d. Eddy covariance measurement of biogenic oxygenated VOC emissions from hay harvesting. Atmos Environ 35:491–495.

Karl T, Guenther A, Lindinger C, Jordan A, Fall R, Lindinger W. 2001e. Eddy covariance measurements of oxygenated volatile organic compound fluxes from crop harvesting using a redesigned proton-transfer-reaction mass spectrometer. J Geophysical Res Atmos 106:24157–24167.

Karl T, Spirig C, Rinne J, Stroud C, Prevost P, Greenberg J, Fall R, Guenther A. 2002. Virtual disjunct eddy covariance measurements of organic compound fluxes from a subalpine forest using proton transfer reaction mass spectrometry. Atmos Chem Phys 2:279–291.

Karl T, Jobson T, Kuster WC, Williams E, Stutz J, Shetter R, Hall SR, Goldan P, Fehsenfeld F, Lindinger W. 2003. Use of proton-transfer-reaction mass spectrometry to characterize volatile organic compound sources at the La Porte super site during the Texas Air Quality Study 2000. J Geophysical Res Atmos 108 doi:10.1029/2002JD003333.

Karl T, Potosnak M, Guenther A, Clark D, Walker J, Herrick JD, Geron C. 2004. Exchange processes of volatile organic compounds above a tropical rain forest: Implications for modeling tropospheric chemistry above dense vegetation. J Geophysical Res Atmos 109 doi:10.1029/2004JD004738.

Karl T, Harren F, Warneke C, de Gouw J, Grayless C, Fall R. 2005. Senescing grass crops as regional sources of reactive volatile organic compounds. J Geophysical Res Atmos 110 doi:10.1029/2005JD005777.

Kato S, Miyakawa Y, Kaneko T, Kajii Y. 2004. Urban air measurements using PTR-MS in Tokyo area and comparison with GC-FID measurements. Int J Mass Spectrom 235:103–110.

Kormann R, Fischer H, de Reus M, Lawrence M, Bruhl C, von Kuhlmann R, Holzinger R, Williams J, Lelieveld J, Warneke C, de Gouw J, Heland J, Ziereis H, Schlager H. 2003. Formaldehyde over the eastern Mediterranean during MINOS: Comparison of airborne in-situ measurements with 3D-model results. Atmos Chem Phys 3:851–861.

Kuster WC, Jobson BT, Karl T, Riemer D, Apel E, Goldan PD, Fehsenfeld FC. 2004. Intercomparison of volatile organic carbon measurement techniques and data at la porte during the TexAQS2000 Air Quality Study. Environ Sci Technol 38:221–228.

Lau YK, Ikuta S, Kebarle P. 1982. Thermodynamics and kinetics of the gas-phase reactions—$H_3O^+(H_2O)_{n-1} + H_2O = H_3O^+(H_2O)_n$. J Am Chem Soc 104:1462–1469.

Lee A, Schade GW, Holzinger R, Goldstein AH. 2005. A comparison of new measurements of total monoterpene flux with improved measurements of speciated monoterpene flux. Atmos Chem Phys 5:505–513.

Lelieveld J, Crutzen PJ, Ramanathan V, Andreae MO, Brenninkmeijer CAM, Campos T, Cass GR, Dickerson RR, Fischer H, de Gouw JA, Hansel A, Jefferson A, Kley D, de Laat ATJ, Lal S, Lawrence MG, Lobert JM, Mayol-Bracero OL, Mitra AP, Novakov T, Oltmans SJ, Prather KA, Reiner T, Rodhe H, Scheeren HA, Sikka D, Williams J. 2001. The indian ocean experiment: Widespread air pollution from South and Southeast Asia. Science 291:1031–1036.

Lelieveld J, Berresheim H, Borrmann S, Crutzen PJ, Dentener FJ, Fischer H, Feichter J, Flatau PJ, Heland J, Holzinger R, Korrmann R, Lawrence MG, Levin Z, Markowicz KM, Mihalopoulos N, Minikin A, Ramanathan V, de Reus M, Roelofs GJ, Scheeren HA, Sciare J, Schlager H, Schultz M, Siegmund P, Steil B, Stephanou EG, Stier P, Traub M, Warneke C, Williams J, Ziereis H. 2002. Global air pollution crossroads over the Mediterranean. Science 298:794–799.

Lewis AC, Hopkins JR, Carpenter LJ, Stanton J, Read KA, Pilling MJ. 2005. Sources and sinks of acetone, methanol, and acetaldehyde in North Atlantic marine air. Atmos Chem Phys 5:1963–1974.

Lide DR. 2005. CRC handbook of chemistry and physics. Boca Raton, FL: CRC Press.

Lindinger W, Fall R, Karl TG. 2001. Environmental, food and medical applications of proton-transfer-reaction mass spectrometry (PTR-MS). Volume 4 of book series, Adams NG, Babcock LM, editors. Advances in Gas-Phase Ion Chemistry. Amsterdam: Elsevier. p 1–48.

Lindinger W, Hansel A, Jordan A. 1998. On-line monitoring of volatile organic compounds at pptv levels by means of proton-transfer-reaction mass spectrometry (PTR-MS)—Medical applications, food control and environmental research. Int J Mass Spectrom 173:191–241.

Midey AJ, Arnold ST, Viggiano AA. 2000. Reactions of $H_3O^+(H_2O)_n$ with formaldehyde and acetaldehyde. J Phys Chem A 104:2706–2709.

Midey AJ, Williams S, Arnold ST, Viggiano AA. 2002. Reactions of $H_3O^+(H_2O)(0,1)$ with alkylbenzenes from 298 to 1200 K. J Phys Chem A 106:11726–11738.

Morrison GC, Howard CJ. 2001. Selective detection of gas-phase aldehydes and ketones using protonated hydrazine. Int J Mass Spectrom 210(211): 503–509.

Northway MJ, de Gouw JA, Fahey DW, Gao RS, Warneke C, Roberts JM, Flocke F. 2004. Evaluation of the role of heterogeneous oxidation of alkenes in the detection of atmospheric acetaldehyde. Atmos Environ 38:6017–6028.

Novakov T, Penner JE. 1993. Large contribution of organic aerosols to cloud-condensation-nuclei concentrations. Nature 365:823–826.

Nowak JB, Parrish DD, Neuman JA, Holloway JS, Cooper OR, Ryerson TB, Nicks DK, Flocke F, Roberts JM, Atlas E, de Gouw JA, Donnelly S, Dunlea E, Hubler G, Huey LG, Schauffler S, Tanner DJ, Warneke C, Fehsenfeld FC. 2004. Gas-phase chemical characteristics of Asian emission plumes observed during ITCT 2K2 over the eastern North Pacific Ocean. J Geophysical Res Atmos 109 doi:10.1029/2003JD004488.

Poschl U, Williams J, Hoor P, Fischer H, Crutzen PJ, Warneke C, Holzinger R, Hansel A, Jordan A, Lindinger W, Scheeren HA, Peters W, Lelieveld J. 2001. High acetone concentrations throughout the 0–12 km altitude range over the tropical rainforest in Surinam. J Atmos Chem 38:115–132.

Prazeller P, Palmer PT, Boscaini E, Jobson T, Alexander M. 2003. Proton transfer reaction ion trap mass spectrometer. Rapid Commun Mass Spectrom 17:1593–1599.

Rinne HJI, Ruuskanen TM, Reissell A, Taipale R, Hakola H, Kulmala M. 2005. On-line PTR-MS measurements of atmospheric concentrations of volatile organic compounds in a European boreal forest ecosystem. Boreal Environ Res 10:425–436.

Roberts JM, Flocke F, Chen G, de Gouw J, Holloway JS, Hubler G, Neuman JA, Nicks DK, Nowak JB, Parrish DD, Ryerson TB, Sueper DT, Warneke C, Fehsenfeld FC. 2004. Measurement of peroxycarboxylic nitric anhydrides (PANs) during the ITCT 2K2 aircraft intensive experiment. J Geophysical Res Atmos 109 doi:10.1029/2004JD004960.

Sanhueza E, Holzinger R, Kleiss B, Donoso L, Crutzen PJ. 2004. New insights in the global cycle of acetonitrile: Release from the ocean and dry deposition in the tropical savanna of Venezuela. Atmos Chem Phys 4:275–280.

Scheeren HA, Lelieveld J, Roelofs GJ, Williams J, Fischer H, de Reus M, de Gouw JA, Warneke C, Holzinger R, Schlager H, Klupfel T, Bolder M, van der Veen C, Lawrence M. 2003. The impact of monsoon outflow from India and Southeast Asia in the upper troposphere over the eastern Mediterranean. Atmos Chem Phys 3:1589–1608.

Singh HB, Chen Y, Staudt A, Jacob D, Blake D, Heikes B, Snow J. 2001. Evidence from the Pacific troposphere for large global sources of oxygenated organic compounds. Nature 410:1078–1081.

Singh HB, Tabazadeh A, Evans MJ, Field BD, Jacob DJ, Sachse G, Crawford JH, Shetter R, Brune WH. 2003. Oxygenated volatile organic chemicals in the oceans: Inferences and implications based on atmospheric observations and air-sea exchange models. Geophysical Res Lett 30 doi:10.1029/2003GL017933.

Smith D, Spanel P. 2005. Selected ion flow tube mass spectrometry (SIFT-MS) for on-line trace gas analysis. Mass Spectrom Rev 24: 661–700.

Spanel P, Ji YF, Smith D. 1997. SIFT studies of the reactions of H_3O^+, NO^+ and O_2^+ with a series of aldehydes and ketones. Int J Mass Spectrom 165:25–37.

Spanel P, Van Doren JM, Smith D. 2002. A selected ion flow tube study of the reactions of H_3O^+, NO^+, and O_2^+ with saturated and unsaturated aldehydes and subsequent hydration of the product ions. Int J Mass Spectrom 213:163–176.

Spanel P, Wang TS, Smith D. 2004. Quantification of hydrogen cyanide in humid air by selected ion flow tube mass spectrometry. Rapid Commun Mass Spectrom 18:1869–1873.

Spanel P, Smith D. 1997. SIFT studies of the reactions of H_3O^+, NO^+ and O_2^+ with a series of alcohols. Int J Mass Spectrom 167:375–388.

Spanel P, Smith D. 1998a. Selected ion flow tube studies of the reactions of H_3O^+ NO^+, and O_2^+ with several aromatic and aliphatic hydrocarbons. Int J Mass Spectrom 181:1–10.

Spanel P, Smith D. 1998b. SIFT studies of the reactions of H_3O^+, NO^+ and O_2^+ with a series of volatile carboxylic acids and esters. Int J Mass Spectrom 172:137–147.

Spanel P, Smith D. 1999. Selected ion flow tube studies of the reactions of H_3O^+, NO^+, and O_2^+ with some chloroalkanes and chloroalkenes. Int J Mass Spectrom 184:175–181.

Spanel P, Diskin AM, Wang T, Smith D. 2003. A SIFT study of the reactions of H_3O^+, NO^+ and O_2^+ with hydrogen peroxide and peroxyacetic acid. Int J Mass Spectrom 228:269–283.

Sprung D, Jost C, Reiner T, Hansel A, Wisthaler A. 2001. Acetone and acetonitrile in the tropical Indian Ocean boundary layer and free troposphere: Aircraft-based intercomparison of AP-CIMS and PTR-MS measurements. J Geophysical Res Atmos 106:28511–28527.

Steinbacher M, Dommen J, Amman C, Spirig C, Neftel A, Prevot A. 2004. Performance characteristics of a proton-transfer-reaction mass spectrometer (PTR-MS) derived from laboratory and field measurements. Int J Mass Spectrom 239:117–128.

Su T, Chesnavich WJ. 1982. Parametrization of the ion-polar molecule collision rate constant by trajectory calculations. J Chem Phys 76:5183–5185.

Tani A, Hayward S, Hansel A, Hewitt CN. 2004. Effect of water vapour pressure on monoterpene measurements using proton transfer reaction-mass spectrometry (PTR-MS). Int J Mass Spectrom 239:161–169.

Traub M, Fischer H, de Reus M, Kormann R, Heland J, Ziereis H, Schlager H, Holzinger R, Williams J, Warneke C, de Gouw J, Lelieveld J. 2003. Chemical characteristics assigned to trajectory clusters during the MINOS campaign. Atmos Chem Phys 3:459–468.

Viehland LA, Mason EA. 1995. Transport properties of gaseous-ions over a wide energy-range. 4. Atomic Data and Nuclear Data Tables 60:37–95.

Viggiano AA, Morris RA. 1996. Rotational and vibrational energy effects on ion-molecule reactivity as studied by the VT-SIFDT technique. J Phys Chem 100:19227–19240.

Wang TS, Spanel P, Smith D. 2003. Selected ion flow tube, SIFT, studies of the reactions of H_3O^+, NO^+ and O_2^+ with eleven $C_{10}H_{16}$ monoterpenes. Int J Mass Spectrom 228:117–126.

Warneke C, de Gouw JA. 2001. Organic trace gas composition of the marine boundary layer over the northwest Indian Ocean in April 2000. Atmos Environ 35:5923–5933.

Warneke C, Holzinger R, Hansel A, Jordan A, Lindinger W, Poschl U, Williams J, Hoor P, Fischer H, Crutzen PJ, Scheeren HA, Lelieveld J. 2001a. Isoprene and its oxidation products methyl vinyl ketone, methacrolein, and isoprene related peroxides measured online over the tropical rain forest of Surinam in March 1998. J Atmos Chem 38:167–185.

Warneke C, van der Veen C, Luxembourg S, de Gouw JA, Kok A. 2001b. Measurements of benzene and toluene in ambient air using proton-transfer-reaction mass spectrometry: Calibration, humidity dependence, and field intercomparison. Int J Mass Spectrom 207: 167–182.

Warneke C, Luxembourg SL, de Gouw JA, Rinne HJI, Guenther AB, Fall R. 2002. Disjunct eddy covariance measurements of oxygenated volatile organic compounds fluxes from an alfalfa field before and after cutting. J Geophysical Res Atmos 107 doi:10.1029/2001JD000594.

Warneke C, De Gouw JA, Kuster WC, Goldan PD, Fall R. 2003. Validation of atmospheric VOC measurements by proton-transfer-reaction mass spectrometry using a gas-chromatographic preseparation method. Environ Sci Technol 37:2494–2501.

Warneke C, de Gouw JA, Goldan PD, Kuster WC, Williams EJ, Lerner BM, Jakoubek R, Brown SS, Stark H, Aldener M, Ravishankara AR, Roberts JM, Marchewka M, Bertman S, Sueper DT, McKeen SA, Meagher JF, Fehsenfeld FC. 2004a. Comparison of daytime and nighttime oxidation of biogenic and anthropogenic VOCs along the New England coast in summer during New England Air Quality Study 2002. J Geophysical Res Atmos 109:D10309 doi:10.1029/2003JD004424.

Warneke C, Rosen S, Lovejoy ER, de Gouw JA, Fall R. 2004b. Two additional advantages of proton-transfer ion trap mass spectrometry. Rapid Commun Mass Spectrom 18:133–134.

Warneke C, de Gouw JA, Lovejoy ER, Murphy PC, Kuster WC, Fall R. 2005a. Development of proton-transfer ion trap-mass spectrometry: On-line detection and identification of volatile organic compounds in air. J Am Soc Mass Spectrom 16:1316–1324.

Warneke C, Kato S, De Gouw JA, Goldan PD, Kuster WC, Shao M, Lovejoy ER, Fall R, Fehsenfeld FC. 2005b. Online volatile organic compound measurements using a newly developed proton-transfer ion-trap mass spectrometry instrument during New England Air Quality Study—Intercontinental Transport and Chemical Transformation 2004: Performance, intercomparison, and compound identification. Environ Sci Technol 39:5390–5397.

Warneke C, de Gouw JA, Stohl A, Cooper OR, Goldan PD, Kuster WC, Holloway JS, Williams EJ, Lerner BM, McKeen SA, Trainer M, Fehsenfeld FC, Atlas EL, Donnelly SG, Stroud V, Lueb A, Kato S. 2006. Biomass burning and anthropogenic sources of CO over New England in the summer 2004. J Geophysical Res Atmos 111: D23S15 doi: 10.1029/2005JD006878.

Wert BP, Trainer M, Fried A, Ryerson TB, Henry B, Potter W, Angevine WM, Atlas E, Donnelly SG, Fehsenfeld FC, Frost GJ, Goldan PD, Hansel A, Holloway JS, Hubler G, Kuster WC, Nicks DK, Neuman JA, Parrish DD, Schauffler S, Stutz J, Sueper DT, Wiedinmyer C, Wisthaler A. 2003. Signatures of terminal alkene oxidation in airborne formaldehyde measurements during TexAQS 2000. J Geophysical Res Atmos 108 doi:10.1029/2002JD002502.

Williams J, Fischer H, Harris GW, Crutzen PJ, Hoor P, Hansel A, Holzinger R, Warneke C, Lindinger W, Scheeren B, Lelieveld J. 2000. Variability-lifetime relationship for organic trace gases: A novel aid to compound identification and estimation of HO concentrations. J Geophysical Res Atmos 105:20473–20486.

Williams J, Poschl U, Crutzen PJ, Hansel A, Holzinger R, Warneke C, Lindinger W, Lelieveld J. 2001. An atmospheric chemistry interpretation of mass scans obtained from a proton transfer mass spectrometer flown over the tropical rainforest of Surinam. J Atmos Chem 38:133–166.

Williams J, Holzinger R, Gros V, Xu X, Atlas E, Wallace DWR. 2004. Measurements of organic species in air and seawater from the tropical Atlantic. Geophysical Res Lett 31 doi:10.1029/2004GL020012.

Wisthaler A, Hansel A, Dickerson RR, Crutzen PJ. 2002. Organic trace gas measurements by PTR-MS during INDOEX 1999. J Geophysical Res Atmos 107 doi:10.1029/2001JD000576.

Wisthaler A, Hansel A, Kleffmann J, Brauers T, Rohrer F, Wahner A. 2003. Real-time detection of nitrous acid (HONO) by PTR-MS: a comparison with LOPAP measurement in the atmosphere simulation chamber SAPHIR. Geophysical Res Abstr 5:00402.

Zare R, Fernandez F, Kimmel J. 2003. Hadamard transform time-of-flight mass spectrometry: More signal, more of the time. Angew Chem Int Ed 42:30–35.

Zhao J, Zhang R. 2004. Proton transfer reaction rate constants between hydronium ion (H_3O^+) and volatile organic compounds. Atmos Environ 38:2177–2185.

Joost de Gouw received his Ph.D. in Physics from the University of Utrecht in the Netherlands in 1994. His thesis research, under supervision of Prof. Henk Heideman, involved measurements of Auger and photoelectrons following the inner-shell ionization of atoms and molecules by synchrotron radiation. Between 1994 and 1997, he was a postdoc with Prof. Steve Leone at the Joint Institute for Laboratory Astrophysics (JILA) in Boulder, Colorado, and worked on cluster ion mobilities and ion-molecule reactions. In 1997, he joined the NOAA Aeronomy Laboratory, and worked with Dr. Carl Howard on the kinetics of radical and surface reactions in the atmosphere using chemical ionization mass spectrometry. He also built a laboratory PTR-MS instrument and used it to study the VOCs from drying vegetation. Between 1999 and 2001, he was an assistant research professor with the Institute for Marine and Atmospheric Research (IMAU) at the University of Utrecht, working on aircraft measurements of VOCs using PTR-MS. In 2001, he rejoined the NOAA Aeronomy Lab, since then renamed NOAA Earth System Research Laboratory, continuing his work on atmospheric VOCs.

Carsten Warneke received his Ph.D. in Physics from the University of Innsbruck in Austria in 1998. His thesis research, under supervision of Prof. Werner Lindinger discussed biogenic volatile organic compound (VOC) emissions from the rain forest in Surinam and the emissions of dead bio-matter by a-biological processes. Between 1999 and 2001, he was post-doc with Prof. Jos Lelieveld and Dr. Joost de Gouw at the University of Utrecht in the Netherlands, where he worked on aircraft and ship-based measurements

of VOCs using PTR-MS over the Indian Ocean and the Mediterranean Sea. In 2001, he joined the NOAA Aeronomy Laboratory, since then renamed NOAA Earth System Research Laboratory, as a research scientist continuing to work on atmospheric VOCs. He also developed a PIT-MS instrument that is used for ship and ground-based measurements of VOCs.